using a *pyr1*-specific DNA probe, which carried the partial *pyr1*, *pyr3*, and *pyr6/pyr5* but lacked *pyr2/pyr4* (Fig. 1). In contrast to *P. caudatus*, we could not detect the full *pyr* gene cluster in *N. saliens*. Amplification of *N. saliens* genomic DNA using primers for *pyr1* and *pyr2/pyr4* or hybridization of the *pyr1*-positive clone with the probe corresponding to the 2 kb upstream region of *pyr2/pyr4* did not yield any positive signals (data not shown).

The Common Evolutionary Origin of the *pyr* Gene Cluster in Trypanosomatids and Bodonids

We previously showed that *pyr2*, *pyr4*, and *pyr6/pyr5* have the same evolutionary origin in trypanosomatids and bodonids (Annoura et al. 2005; Makiuchi et al. 2007). We further assessed whether the other *pyr* genes, *pyr1* and *pyr3*, have a common evolutionary origin in kinetoplastids.

Pyr1 of both trypanosomatids and bodonids were found to have the same protein structure, comprised of an N-terminal GAT domain, a linker, and a C-terminal CPS domain (Supplementary Fig. S1). Phylogenetic reconstruction of the CPS domain of pyr1 showed monophyly of the trypanosomatid and bodonid pyr1, with strong bootstrap support (99% in the maximum likelihood (ML) method, Supplementary Fig. S2).

In the pyr3 tree, a monophyletic grouping of kinetoplastids was also supported (85% in ML, Supplementary Fig. S3). Importantly, the amino acid sequence alignment of pyr3 from various species showed kinetoplastid-specific amino acid insertions (Fig. 2). These results indicate that the *pyr1* and *pyr3* genes, as well as *pyr2*, *pyr4*, and *pyr6/pyr5*, have the same origin in trypanosomatids and bodonids.

Although the organization of *pyr1*, *pyr2*, and *pyr3* in non-kinetoplastid euglenozoans is unclear, these genes are likely to be independent, as well as kinetoplastids. We found that *Naegleria gruberi*, which belongs to Heterolobosea, the closest group to Euglenozoa, possesses an independent *pyr3*. In addition, an independent *pyr2* was found in the *N. gruberi* genome sequence database (data not shown). These findings are consistent with the notion that gene fusion of pyr1/pyr3/pyr2 (CAD) is present in unikonts but absent from bikonts (Stechmann and Cavalier-Smith 2003), with the exception of a red algal CAD (Nozaki et al. 2005).

The Different Origin of the *pyr4* Gene in Kinetoplastids and Diplonemids

We addressed whether the *pyr* gene cluster is present in diplonemids, which are most closely related to kinetoplastids. Although we performed cDNA-PCR cloning using various sets of degenerated primers for all *pyr* genes in the diplonemid, *D. papillatum*, we obtained PCR products only for pyr4 and pyr6.

Pyr4 enzymes have been classified into three types: family-1A, -1B, and -2 enzymes. Family-2 pyr4 is present in the euglenoid, *Euglena gracilis*, and in many eukaryotic groups, whereas family-1A pyr4, which originated via LGT, is present in kinetoplastids (Annoura et al. 2005). Using *D. papillatum* RNA as a template, we obtained cDNA-PCR products using primers specific for family-2, but not for family-1A, pyr4.

We found that an open reading frame of *D. papillatum* pyr4 cDNA encoded for 395 amino acids, with the predicted amino acid sequence

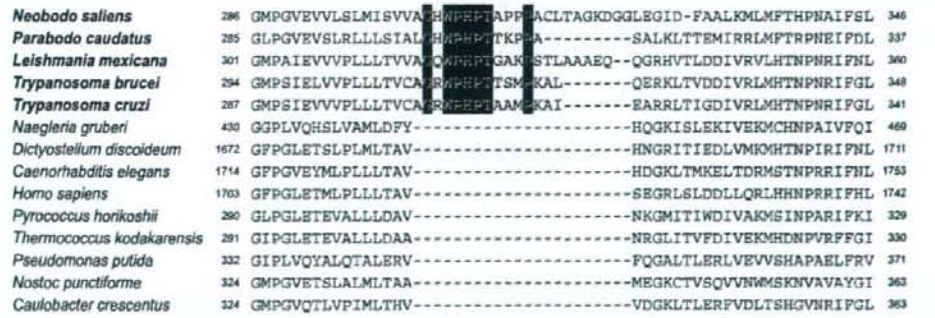

Figure 2. Alignment of pyr3 sequences among various species. The kinetoplastid-specific insertions are shaded. Within this region, the amino acid sequence motif, GXWPHPTXXXP, is fully conserved in kinetoplastids and shown in black boxes.

(A)

	Type of DHOD		FMN site	Orotate site
Family 2				
	diplonemids	*Diplonema papillatum*	GFGFVEI**C**TVTPLPQP	YIVINVSSPNTPGLR
	euglenoids	*Euglena gracilis*	GFGFVEI**C**TVTPLPQP	YLVINVSSPNTPGLR
	Metazoa	*Homo sapiens*	GFGFVEI**C**SVTPKPQE	YLVVNVSSPNTAGLR
	Viridiplantae	*Arabidopsis thaliana*	GFGFVEV**C**SVTPVPQE	YLVINVSSPNTAGLR
	Fungi	*Schizosaccharomyces pombe*	GFSYLEI**C**SVTPKPQP	ILVINVSSPNTPGLR
Family 1A				
	trypanosomatids	*Trypanosoma cruzi*	SSGALVS**K**SCTSAPRD	LLELNLSCPNVPGKP
	bodonids	*Parabodo caudatus*	SSGSLIT**K**SCTSAFRE	ILELNLSCPNVPGKP
		Neobodo saliens	ASGTLIT**K**SCTAQQRD	LLELNLSCPNVPGKP
	Fungi	*Saccharomyces cerevisiae*	KAGAFIT**K**SATTLERE	ITELNLSCPNVPGKP
	Firmicutes	*Lactococcus lactis* A	QAGAYIT**K**SSTLEKRE	ITELNLSCPNVPGKP

(B)

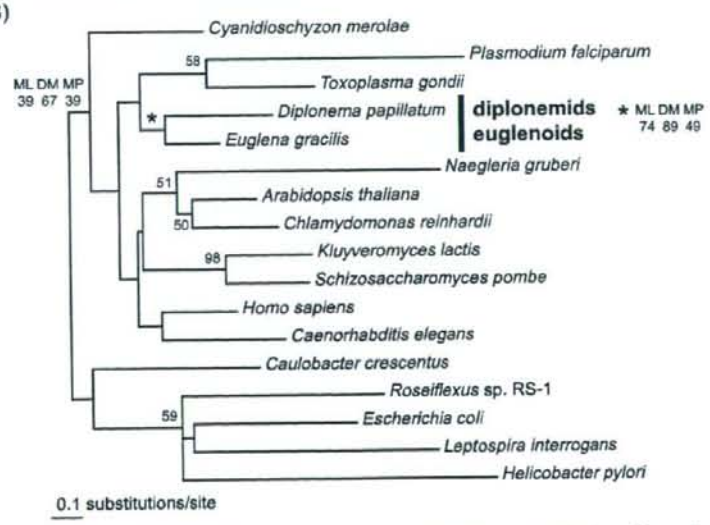

Figure 3. Amino acid sequence comparison and phylogenetic analysis of pyr4. (**A**) Amino acids indispensable for binding of flavin mononucleotide (FMN) (black boxes) and orotate (gray boxes) in family-2 and -1A type pyr4. (**B**) Phylogenetic analysis of family-2 pyr4. The consensus tree of the maximum likelihood (ML) method with 100 replicates is shown. The tree was inferred by the JTT model taking across-site rate heterogeneity into consideration. The α-value of the Γ-shaped parameter used in the analysis was 0.63597. Bootstrap proportion (BP) values are attached to the internal branches. Branches with less than 50% BP support are unmarked. BP values for a diplonemids/euglenoids clade are marked by an asterisk and given by ML, distance matrix (DM), and maximum parsimony (MP) methods. The length of each branch is proportional to the estimated number of substitutions. With 17 taxa, 230 unambiguously aligned amino acid sites were used for analysis, corresponding to residues 81—105, 107—157, 166—174, 179—225, 240—250, 255—260, 265—28w1, 290—308, and 317—361 of the *Diplonema papillatum* sequence.

sharing a higher identity to that of *E. gracilis* (51%) than those of kinetoplastids (18—26%). The amino acid residues of *D. papillatum* pyr4 used for binding of flavin mononucleotide and orotate were of family-2 type (Fig. 3A). These results clearly indicate that *D. papillatum* possesses the family-2 *pyr4* gene. Phylogenetic analysis of family-2 pyr4 showed monophyly of euglenoids and diplonemids, whereas the bootstrap support was moderate (74% in ML, Fig. 3B). In conjunction with the monophyletic grouping of kinetoplastid pyr4 (Annoura et al. 2005), we conclude that the origin of *pyr4* is different between kinetoplastids and euglenoids/diplonemids.

Different Organization of *pyr5* and *pyr6* Genes in Euglenozoa

The *pyr5* and *pyr6* genes have a different gene structure in euglenoids and kinetoplastids. *E. gracilis* possesses a fused *pyr5/pyr6* gene, whereas, in kinetoplastids, the genes are inversely fused as *pyr6/pyr5* (Makiuchi et al. 2007).

We found that the *D. papillatum* pyr6 cDNA encoded for 271 amino acids and retained spliced leader and poly(A) sequences at its 5′- and 3′-termini, respectively (data not shown). These results indicate that the cloned *D. papillatum* pyr6 cDNA is not truncated, but is a mature form of the transcript. In addition, we could not detect any clone in which pyr6 was fused with the pyr5 sequence, suggesting that *D. papillatum* has stand-alone genes for pyr6 and probably for pyr5.

Phylogenetic analysis of pyr6 reconstructed a monophyletic grouping of *D. papillatum* pyr6 and the pyr6 domain of *E. gracilis* pyr5/pyr6 within a eukaryotic clade with 82% bootstrap support (ML analysis) (Fig. 4). Interestingly, Apicomplexa and Fungi, also possess a stand-alone *pyr6*, whereas these eukaryotic groups are phylogenetically distantly related to diplonemids (Makiuchi et al. 2007). The apicomplexan pyr6 clustered with the kinetoplastid pyr6/pyr5 in the bacterial clade to the exclusion of *D. papillatum* pyr6 with strong bootstrap support (99% in ML, Fig. 4), indicating that the origin of *pyr6* is different between Apicomplexa and diplonemids.

D. papillatum and fungal pyr6 were nested in the eukaryotic clade. To determine whether diplonemid and fungal *pyr6* have the same origin, we performed an approximately unbiased (AU) test in terms of statistical comparisons of the alternative trees, in which diplonemid or fungal *pyr6* was

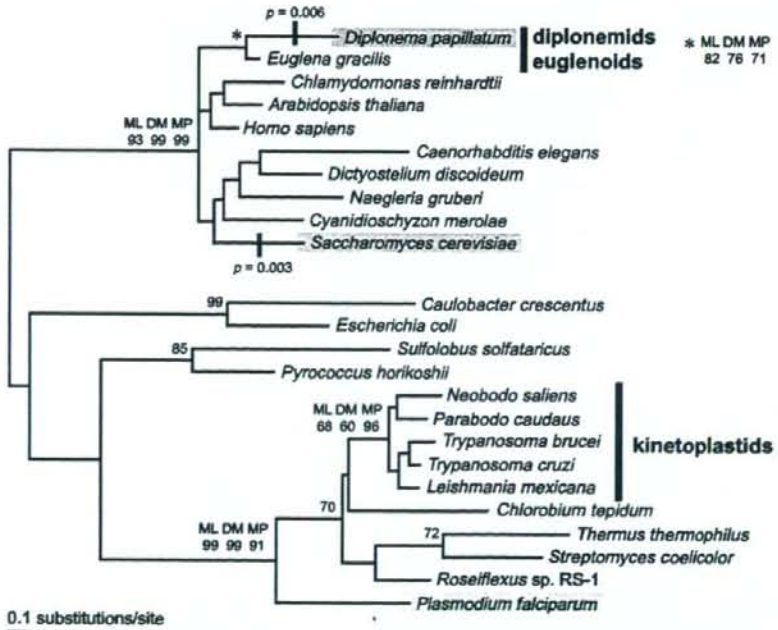

Figure 4. Bootstrap consensus tree of the ML method with 100 replicates for pyr6. The tree was inferred by the JTT model taking across-site rate heterogeneity into consideration. The α-value of the Γ-shaped parameter used in the analysis was 1.11259. The eukaryotic species having stand-alone pyr6 are shaded. Methods and labeling are as in Figure 3. Analysis involved 118 unambiguously aligned amino acid sites with 24 taxa, corresponding to residues 32–39, 43–71, 87–100, 114–125, 142–155, 173–181, 192–200, 202–205, and 219–237 of the *D. papillatum* sequence.

grafted to either branch in the tree in Figure 4. The alternative trees grafting the fungal sequence to the diplonemid branch and vice versa were statistically significantly different from the tree in Figure 4 with $p = 0.006$ and 0.003, respectively, indicating that the diplonemid and fungal *pyr6* do not have the same origin. Thus, these findings strongly suggest that the euglenoid and diplonemid *pyr6* genes share a common evolutionary origin, despite the different gene organization, and that the secondary split of the *pyr5/pyr6* gene likely occurred on the line leading to *D. papillatum* after its separation from the line leading to euglenoids, although the nature of the diplonemid *pyr5* gene is not yet known.

Discussion

The unity of kinetoplastids, diplonemids, and euglenoids in Euglenozoa has been evidenced by their morphology, protein phylogeny, and mitochondrial properties. For example, all euglenozoans share a unique mitochondrial DNA structure, with the mitochondrial genome comprised of multiple copies of circular DNAs (Marande et al. 2005; Roy et al. 2007). Although these findings emphasize the uniqueness of Euglenozoa among the eukaryotic groups, paradoxically, the taxonomic boundaries of the euglenozoan groups became rather obscure. Thus, our results shed new light on the critical evolutionary gap between kinetoplastids and diplonemids/euglenoids by analyses of the synteny and gene fusion of *pyr* genes.

Conserved Synteny of *pyr* Genes in Kinetoplastids

We presented evidence for the presence of the *pyr* gene cluster in the bodonid, *P. caudatus*, strongly suggesting that the *pyr* gene cluster was established in a common ancestor of trypanosomatids and bodonids. This finding is also supported by the partial clustering of the *pyr1*, *pyr3*, and *pyr6/pyr5* genes and the occurrence of the *pyr2/pyr4* gene fusion, in *N. saliens* (Fig. 1). The presence of the fused *pyr2/pyr4* gene appears to reflect an evolutionary trait, which may have resulted from the loss of the untranslated region between *pyr2* and *pyr4* genes (Annoura et al. 2005). Failure to detect the full *pyr* gene cluster in *N. saliens* may be due to the presence of the long intervening sequence between the *pyr6/pyr5* and *pyr2/pyr4* genes, a sequence too long for PCR amplification. Another possibility is the occurrence of the rearrangement of the *pyr* gene cluster, as in *T. cruzi*, in which the partially amplified *pyr* gene clusters were frequently detected (Nara et al. 2003).

Genome reduction has been frequently observed in endosymbionts and parasitic microbes, accompanied by loss of both genes and non-coding regions (Dobrindt et al. 2004; Gross et al. 2003; Moran 2002; van Ham et al. 2003). We have shown here that, compared with the parasitic trypanosomatids, the free-living *P. caudatus* has shorter untranslated regions between the *pyr* genes (Fig. 1). This discrepancy may be explained by the possible compact nature of the bodonid genomes. Comparative genomics between trypanosomatids and free-living bodonids would clarify this point.

The Timing of Lateral Gene Transfer of *pyr* Genes Pinpointed

We were able to identify *pyr4* and *pyr6* genes in *D. papillatum*, thus allowing us to examine their molecular phylogeny in the euglenozoan groups.

The *pyr4* gene: Since the family-1A pyr4 of trypanosomatids has biochemical properties different from that of the family-2 pyr4 of canonical eukaryotes, including human, pyr4 may be a promising target for chemotherapy against trypanosomiasis (Nara et al. 2005). The family-1A *pyr4* gene in kinetoplastids was shown to have originated from anaerobic microbes via LGT, whereas an ancestral eukaryote may have acquired the family-2 *pyr4* from mitochondria (Annoura et al. 2005). We found that euglenoid and diplonemid pyr4 were both nested within the family-2 clade to the exclusion of the kinetoplastid sequences of family-1A type. Together with the finding that most eukaryotic groups, including Heterolobosea, the closest group to Euglenozoa, possess family-2 pyr4 (Arisue et al. 2005; Nara et al. 2000; Rodríguez-Ezpeleta et al. 2007; Simpson et al. 2006a), these results pinpoint the timing of LGT of *pyr4* to a common ancestor of kinetoplastids after separation of the lines leading to euglenoids and diplonemids (Fig. 1).

The *pyr6* gene: Similar to *pyr4*, the kinetoplastid *pyr6* gene was shown to have a prokaryotic origin and to have been acquired via LGT (Makiuchi et al. 2007; Nara et al. 2000). In *D. papillatum*, the presence of a stand-alone *pyr6* gene was unexpected, because euglenoids and the group Heterolobosea, which share a

common ancestor, possess fused *pyr5/pyr6* genes. In our phylogenetic analysis, the stand-alone *pyr6* gene of *D. papillatum* was grouped with the pyr6 domain of euglenoid *pyr5/pyr6*, but not with the stand-alone genes of Apicomplexa and Fungi (Fig. 4). It is important to note that apicomplexan *pyr6* has been shown to originate via LGT (Makiuchi et al. 2007). In addition, our AU test rejected the monophyly of diplonemid and fungal pyr6 (this study). These findings indicate that the diplonemid *pyr6* was not derived from apicomplexan or fungal *pyr6* via LGT. Therefore, it is likely that the diplonemid *pyr6* has the same origin as euglenoid *pyr5/pyr6*. Thus, we conclude that LGT of *pyr6* occurred in a common ancestor of kinetoplastids after separation of the lines leading to euglenoids and diplonemids (Fig. 1).

An Evolutionary Gap between Kinetoplastids and Diplonemids

Due primarily to the lack of sequence information on the *pyr1*, *pyr2*, *pyr3*, and *pyr5* genes, it is unclear whether the *pyr* gene cluster is present in diplonemids. Regarding the organization of *pyr1*, *pyr2*, and *pyr3* in diplonemids and euglenoids, these genes are likely to be independent, as well as in kinetoplastids, because independent *pyr2* and *pyr3* was found in Heterolobosea, which shares a common ancestor with Euglenozoa.

Clustering of *pyr1*, *pyr2*, and *pyr3* may be present in the genomes of diplonemids and euglenoids, which should be clarified by further sequence analysis of *pyr* genes in these groups. On the other hand, clustering of all of the *pyr* genes is likely to have occurred in a common ancestor of kinetoplastids after separation of the line leading to diplonemids. Because the *pyr4* and *pyr6* genes of diplonemids and kinetoplastids do not share high sequence similarity at both nucleotide and amino acid levels, it is difficult to suppose that homologous recombination has occurred between the original and acquired genes within the already established *pyr* gene cluster.

Another possibility for the origin of clustering of *pyr* genes in kinetoplastids is that the *pyr* gene cluster may have originated in other organism(s) and transferred laterally to kinetoplastids. This explanation seems more parsimonious and cannot be entirely excluded. However, it is rather difficult to postulate such hypothetical eukaryotes, which may possess the same mosaic nature of *pyr* genes in their gene organization and evolutionary origin as kinetoplastids do. Likewise, there is no prokaryote having *pyr* genes of a eukaryotic origin in its *pyr* operon. Thus, the *pyr* gene cluster is likely to have been established in a common ancestor of kinetoplastids after separation of the line leading to diplonemids (Fig. 1).

Evolutionary Implications of Synteny in Euglenozoa

Although the *pyr* gene cluster constitutes a part of a large syntenic block in trypanosomatids, it is not yet known whether large-scale synteny is conserved in non-trypanosomatid euglenozoans. More importantly, the occurrence of large-scale synteny, composed of dozens of functionally unrelated genes, raises fundamental questions of how large-scale synteny is maintained and what its biological significance is. Presently, synteny is thought to be significant only as an important evolutionary signal (Bennetzen and Freeling 1997; Nadeau 1989). In general, we may recognize phylogenetic relationships between taxa by the presence of conserved synteny. However, lack of conserved synteny does not necessarily indicate their phylogenetically distant relation.

Because genome architecture varies from species to species, synteny becomes scarce or is lost by accumulation of frequent, species-specific rearrangement of chromosomal DNA, including meiotic DNA recombination. Accordingly, the genomes of trypanosomatids, and probably bodonids, may be more resistant than the genomes of other eukaryotes to chromosomal rearrangements caused by transpositions and reversals of DNA regions, resulting in conservation of large-scale synteny. Actually, conservation of clustering of whole *pyr* genes in kinetoplastids appears to indicate that there is strong selection pressure to maintain both the number and the order of these genes in a syntenic cluster in the genome within this group of organisms. Although the mechanisms used to maintain their genome architecture are not yet known, this assumption is also supported by the occurrence of large polycistronic transcription units in trypanosomatids, which may be interfered by reversals of regions of chromosomal DNA.

Another factor affecting synteny includes the timing of lineage divergence. In trypanosomatids, the estimate time of the origin of *T. cruzi* is $\geqslant$95 million years ago when calibrated by the phylogeny of insects, which are the sole hosts of trypanosomatids (Gaunt and Miles 2002). However, an estimate of the age of divergence of the euglenozoan branches had not been demonstrated, due

exclusively to the lack of appropriate calibration methods for the timing of their branching. The evolutionary gap between kinetoplastids and non-kinetoplastid euglenozoans could be explained by their extremely ancient origins, which should be proven using reliable means of estimate for the divergence time of the euglenozoan branches.

Complex Evolutionary Events of Gene Rearrangement in Euglenozoa

Evolutionarily, the presence of stand-alone *pyr6* in diplonemids, which appears to have the same origin as its euglenoid counterpart, may provide important insights into the evolutionary process of rearrangement of gene fusion. Our previous analyses suggested that the kinetoplastid *pyr6/pyr5* emerged through three evolutionary events: (1) splitting of the original *pyr5/pyr6*, (2) LGT-based acquisition of the *pyr6* gene, and (3) re-fusion between the acquired *pyr6* and the resident *pyr5* genes in the reverse order, although the temporal order of gene splitting and LGT is not clear.

Importantly, diplonemids constitute an intermediate branch between euglenoids and kinetoplastids in Euglenozoa. Therefore, it is likely that the splitting of *pyr5/pyr6* occurred first, in a common ancestor of diplonemids and kinetoplastids, and that, after separation of the diplonemid lineage, a common ancestor of kinetoplastids acquired *pyr6* via LGT, followed by its subsequent re-fusion into *pyr6/pyr5*. Nevertheless, we cannot exclude the possibility that rearrangement of *pyr5/pyr6* occurred independently in the diplonemid and kinetoplastid lineages (Fig. 1).

Structural rearrangements of *pyr5/pyr6* have been shown to accompany LGT events of either or both genes, suggesting that the acquired genes have contributed to the establishment of the rearranged gene structure (Makiuchi et al. 2007). It is important to determine whether diplonemid and euglenoid *pyr5* have common or different evolutionary origins. Further cloning and phylogenetic analysis of the *pyr5* gene in diplonemids would clarify the evolutionary process involved in the rearrangement of the gene fusion.

Concluding Remarks

In the present study, we pinpointed the timing of synteny of the *pyr* gene cluster and LGT of *pyr4* and *pyr6* to a common ancestor of kinetoplastids. We propose the putative evolutionary steps in the transition from *pyr5/pyr6* fusion to inverted *pyr6/pyr5* fusion. Our findings also emphasize the phylogenetic and molecular biological gaps between kinetoplastids and diplonemids/euglenoids. Comparative genomics of these groups are necessary to understand the nature and evolutionary traits of diversification in Euglenozoa.

Methods

Organisms: Monoxenic cultures of *P. caudatus* (ATCC 50361; American Type Culture Collection, Manassas, VA, USA) or *N. saliens* (ATCC 50358) with *Klebsiella pneumoniae* subsp. (ATCC 27889) were routinely maintained as described (Annoura et al. 2005). Axenic cultures of *D. papillatum* (ATCC 50162) were maintained at 25 °C in ATCC medium 1728; the cells were collected by centrifugation at 3000 rpm for 10 min at 4 °C, and washed 3 times by suspension in artificial seawater and centrifugation at 3000 rpm for 10 min at 4 °C.

Nucleic acid extraction: Total RNA was extracted from freshly prepared cells of *P. caudatus*, *N. saliens*, or *D. papillatum* (4.9×10^8 cells) using TRIZOL® reagent (Invitrogen, Carlsbad, San Diego, CA, USA) as described (Annoura et al. 2005). Protist poly(A) RNA was isolated from total RNA using GenElute™ mRNA Miniprep Kits (Sigma-Aldrich Japan, K.K., Japan). For isolation of *P. caudatus* genomic DNA, 1.0×10^9 freshly harvested cells were suspended in TNE buffer (10 mM Tris—HCl, 100 mM NaCl, 2 mM EDTA, pH 7.5) and lysed by adding sodium dodecyl sulfate (SDS) and Proteinase K (Roche Diagnostics K.K., Minato-ku, Tokyo, Japan) to final concentrations of 0.6% and 200 μg/ml, respectively, and incubating the mixtures at 42 °C for 90 h. Cell lysate was extracted with an equivalent volume of phenol saturated with TE buffer (10 mM Tris—HCl, 1 mM EDTA, pH 7.5) for 15 min at room temperature with gentle shaking, followed by centrifugation at 3000 rpm for 10 min at room temperature. The lysate was extracted with chloroform using the same procedure, and total DNA was precipitated with ethanol, dissolved in TE containing 10 μg/ml RNase A, and stored at 4 °C until use.

cDNA cloning of *pyr* genes from Euglenozoa: Using total RNA from *P. caudatus* or *N. saliens*, cDNA was synthesized using SuperScript™ III RNase H⁻ Reverse Transcriptase (Invitrogen) and oligo(dT) primer. The CPS domain of eukaryotic pyr1 was amplified using the outer primer set, pyr1-F1 (5′-CARGCIGGIGARTTYGAYTA-3′, according to the IUB format) and pyr1-R2 (5′-GTIWSIACIGTYTCIGGRTT-3′), followed by a second PCR step (nested PCR) using the inner primer set, pyr1-F2 (5′-GGIGGICARACIGCIYTIAA-3′) and pyr1-R1 (5′-GGRSAICCIGTIGCYTT-3′). The 674 bp PCR product was subcloned in a TA cloning vector and sequenced using an automated DNA sequencer (CEQ™ 8000 Genetic Analysis System, BECKMAN COULTER, Fullerton, CA, USA). *D. papillatum* cDNA, synthesized as above, was used for nested PCR. *D. papillatum* pyr4 cDNA was PCR amplified using the primers pyr4-F1 (5′-GAATTCGCIGCIGGITTYGAY-AA-3′) and pyr4-R2 (5′-GTCGACACIARISWIGCICCIGC-3′), followed by a second amplification using the primers pyr4-F2 (5′-GAATTCATYAAYMGITAYGGITT-3′) and pyr4-R1 (5′-GTC-GACARICCIGGIGTRTTIGG-3′). *D. papillatum* pyr6 cDNA was cloned by PCR amplification using the primers pyr6-F1 (5′-TTYGARGAYMGIAARYTIGC-3′) and pyr6-R2 (5′-DWWIA-YICCICKICCIAC-3′), followed by a second amplification using the primers pyr6-F2 (5′-GCIGAYATHGGIMAIRYIGT-3′) and

pyr6-R1 (5′-GGISWRTYRTAYTGYTGICC-3′). The PCR products were subcloned in pCRII-TOPO vector (Invitrogen) and sequenced.

Rapid amplification of cDNA ends (RACE) of *pyr* genes in Euglenozoa: *P. caudatus* pyr1 cDNA was synthesized using the specific antisense primer (5′-GTGTGAATTCCCATCGGATC-3′). 5′-RACE was carried out using the sense primer (5′-ACTTACGCTATAAAAGATACAGT-3′), which is specific to the spliced leader (SL) sequence of *P. caudatus* (Sturm et al. 2001) and the antisense primer (5′-CTTGACGGACATCTCGATGA-3′). Full-length cDNA of *D. papillatum* pyr4 and pyr6 were cloned by 5′- and 3′-RACE. For 5′-RACE of *D. papillatum* pyr4, cDNA was synthesized using the pyr4-specific antisense primer (5′-ACACGTTGATGACGATGTAG-3′), followed by PCR amplification using the *D. papillatum* SL-specific primer (5′-GCTACAGTTTCTGTACTTTATTG-3′) (Sturm et al. 2001) and the antisense primer (5′-ACCGGGGTCAGGTTGTATTT-3′). For 5′-RACE of *D. papillatum* pyr6, cDNA was synthesized using the pyr6-specific antisense primer (5′-AACCCTGCGTGGTCGGTGAT-3′), followed by PCR amplification using the above SL-specific primer and the antisense primer (5′-ACAATGTGCGCGTTGGTCAC-3′). For 3′-RACE, *D. papillatum* cDNA was synthesized using the oligo(dT)-anchor primer (5′-AATAAAGCGGCCGCGGATCCAATTTTTTTTTTTTTTTTVN-3′), followed by PCR amplification using a single sense primer (5′-GCTTCGTTGAAATCGGCACCGTGAC-3′ for pyr4 or 5′-TGATGCTGCAGTACGAGCACGGCCA-3′ for pyr6) to quantify the cDNA template. The resulting cDNA was PCR amplified using the anchor primer (5′-AATAAAGCGGCCGCGGATCCAA-3′) and the primer specific to pyr4 (5′-CGCATGTGGCGATTGACCGA-3′) or pyr6 (5′-AAATGTCGTCGAAGGGGACGCTCGC-3′). Finally, the full-length pyr4 cDNA was PCR amplified using the specific primers, (5′-CACCATGTTCACTCGGCTGGCTGTGGCTGGGGGA-3′) and (5′-CACCATGCCCGAGCTCTCTTTCCAAGAAC-3′), and full-length pyr6 cDNA was PCR amplified using the specific primers, (5′-CTAGGCCCCCCGCAGGTCACTTGGCATCAG-3′) and (5′-CTACTGAAACATGGCCTTCGGGTAC-3′). Each full-length cDNA was subcloned and sequenced completely. Note that, although sequencing of full-length pyr1 cDNA of *N. saliens* was incomplete because of failure of 5′-RACE, the partial *N. saliens* pyr1 had the same domain structure as the other kinetoplastid ones.

Identification of the *pyr* gene cluster in *P. caudatus*: The *pyr1* and *pyr4* genes are the 5′- and 3′-terminal genes, respectively, of the *pyr* gene cluster in trypanosomatids. If the syntenic *pyr* gene cluster is conserved in bodonids, the other *pyr* genes are likely to be located between *pyr1* and *pyr4*. To identify the *pyr* gene cluster in *P. caudatus*, we separately amplified its 5′-half, including the putative *pyr1-pyr3-pyr6/pyr5*, and its 3′-half including *pyr6/pyr5-pyr2-pyr4*. PCR amplification was performed using the genomic DNA as the template and the pyr1-specific sense primer (5′-CAGATCGGCGAGCATGTTGC-3′) and the pyr6-specific antisense primer (5′-TGAGCCTCTTGAGCCGGATC-3′) for *pyr1-pyr3-pyr6/pyr5* or the pyr5-specific sense primer (5′-CCGTGTTCGAGCAGTCGCTC-3′) and the pyr4-specific antisense primer (5′-GACACGAAAGGTTCAGCTCC-3′) for *pyr6/pyr5-pyr2-pyr4*. The 7 and 3 kb DNA fragments were obtained and found to contain *pyr3* and *pyr2*, respectively. The overlapping 170 bp nucleotides between these 7 and 3 kb PCR fragments showed 100% sequence identity. Finally, the *pyr* gene cluster was completely sequenced.

Phylogenetic analyses: All sequence data, with the exception of those cloned by us and first reported here, were collected from public sequence databases by taxonomic and BLAST searches. The sequences reported in this paper appear in the DDBJ/EMBL/GenBank databases with the accession numbers AB307736 for the *Parabodo caudatus* pyrimidine biosynthetic gene cluster encoding pyr1, pyr3, pyr6/pyr5 fusion protein, pyr2, and pyr4; AB307737 for the *Neobodo saliens* pyrimidine biosynthetic gene cluster encoding pyr1, pyr3, and pyr6/pyr5; AB307738 for *Diplonema papillatum* pyr4 mRNA; and AB307739 for *D. papillatum* pyr6 mRNA. Unpublished sequences were obtained from various genome project databases: DOE Joint Genome Institute (http://genome.jgi-psf.org/) for the green alga, *Chlamydomonas reinhardtii*, the diatom, *Thalassiosira pseudonana*, the heterolobosea, *Naegleria gruberi*, and the oomycete, *Phytophthora sojae*; the *Cyanidioschyzon merolae* Genome Project (http://merolae.biol.s.u-tokyo.ac.jp/) for the red alga, *Cyanidioschyzon merolae*; and ToxoDB (http://toxodb.org/) for the apicomplexan *Toxoplasma gondii*. Multiple alignments for pyr1, pyr3, pyr4, and pyr6 sequences were obtained using CLUSTAL W (Thompson et al. 1994), with the alignments corrected by manual inspection. The amino acid sequence alignments used in the present study are available upon request. Unambiguously aligned positions were selected and used for phylogenetic analyses. The ML, distance matrix (DM), and maximum parsimony (MP) methods for protein phylogeny were applied to the data sets using the CODEML program in PAML3.1 (Yang 1997) and the PROML, PROTDIST, NEIGHBOR, PROTPARS, SEQBOOT, and CONSENSE programs in PHYLIP3.6a, distributed by Dr. Joseph Felsenstein, University of Washington. In ML analysis, an initial tree search was performed by applying PROML with the JTT model for amino acid substitution, assuming homogeneous rates across sites. Based on the optimal tree obtained, the Γ-shaped parameter (α) of the discrete Γ-distribution with four categories that approximated site rates was estimated using CODEML. Using this α-value, a further tree search was performed with the JTT model with four site rate categories using PROML with the global rearrangement option, producing the final optimal tree. In DM analysis, ML estimates for pairwise distances among the sequences analyzed were calculated using PROTDIST, based on the JTT model with rate variation allowed among sites. Then the neighbor-joining (NJ) tree was reconstructed from the distances using NEIGHBOR. In MP analysis, the MP tree was searched using PROTPARS. Bootstrap analysis for each of the three methods was performed in the same way by applying PROML, PROTDIST+NEIGHBOR, or PROTPARS to the resampled data sets produced by SEQBOOT. One hundred and 1000 resamplings were performed for ML and for DM and MP analyses, respectively. A consensus tree was generated using the CONSENSE program based on the bootstrap analysis of the ML method. The AU test (Shimodaira 2002) in the CONSEL program (Shimodaira and Hasegawa 2001) was used for statistical comparisons among the alternative pyr6 trees.

Acknowledgements

This work was supported in part by Grants-in-Aid for Scientific Research (Nos. 17370086, 17390123, 18890188, and 19590436) and for the 21st Century Center of Excellence Research (to Makiuchi, Murata, and Aoki) from the Ministry

of Education, Science, Sports, Culture, and Technology of Japan.

Appendix A. Supplementary materials

Supplementary data associated with this article can be found in the online version at doi:10.1016/j.protis.2008.02.002.

References

Annoura T, Nara T, Makiuchi T, Hashimoto T, Aoki T (2005) The origin of dihydroorotate dehydrogenase genes of kinetoplastids, with special reference to their biological significance and adaptation to anaerobic, parasitic conditions. J Mol Evol **60**: 113–127

Arisue N, Hasegawa M, Hashimoto T (2005) Root of the Eukaryota tree as inferred from combined maximum likelihood analyses of multiple molecular sequence data. Mol Biol Evol **22**: 409–420

Bennetzen JL, Freeling M (1997) The unified grass genome: synergy in synteny. Genome Res **7**: 301–306

Berriman M, Ghedin E, Hertz-Fowler C, Blandin G, Renauld H, Bartholomeu DC, Lennard NJ, Caler E, Hamlin NE, Haas B, Böhme U, Hannick L, Aslett MA, Shallom J, Marcello L, Hou L, Wickstead B, Alsmark UC, Arrowsmith C, Atkin RJ, Barron AJ, Bringaud F, Brooks K, Carrington M, Cherevach I, Chillingworth TJ, Churcher C, Clark LN, Corton CH, Cronin A, Davies RM, Doggett J, Djikeng A, Feldblyum T, Field MC, Fraser A, Goodhead I, Hance Z, Harper D, Harris BR, Hauser H, Hostetler J, Ivens A, Jagels K, Johnson D, Johnson J, Jones K, Kerhornou AX, Koo H, Larke N, Landfear S, Larkin C, Leech V, Line A, Lord A, Macleod A, Mooney PJ, Moule S, Martin DM, Morgan GW, Mungall K, Norbertczak H, Ormond D, Pai G, Peacock CS, Peterson J, Quail MA, Rabbinowitsch E, Rajandream MA, Reitter C, Salzberg SL, Sanders M, Schobel S, Sharp S, Simmonds M, Simpson AJ, Tallon L, Turner CM, Tait A, Tivey AR, Van Aken S, Walker D, Wanless D, Wang S, White B, White O, Whitehead S, Woodward J, Wortman J, Adams MD, Embley TM, Gull K, Ullu E, Barry JD, Fairlamb AH, Opperdoes F, Barrell BG, Donelson JE, Hall N, Fraser CM, Melville SE, El-Sayed NM (2005) The genome of the African trypanosome *Trypanosoma brucei*. Science **309**: 416–422

Bonen L (1993) Trans-splicing of pre-mRNA in plants, animals, and protists. FASEB J **7**: 40–46

Cavalier-Smith T (1981) Eukaryote kingdoms: seven or nine? Biosystems **14**: 461–481

Dávila AM, Lukeš J (2003) Towards a framework for the evolutionary genomics of kinetoplastids: what kind of data and how much? Kinetoplastid Biol Dis **2**: 16

Dobrindt U, Hochhut B, Hentschel U, Hacker J (2004) Genomic islands in pathogenic and environmental microorganisms. Nat Rev Microbiol **2**: 414–424

El-Sayed NM, Myler PJ, Blandin G, Berriman M, Crabtree J, Aggarwal G, Caler E, Renauld H, Worthey EA, Hertz-Fowler C, Ghedin E, Peacock C, Bartholomeu DC, Haas BJ, Tran AN, Wortman JR, Alsmark UC, Angiuoli S, Anupama A, Badger J, Bringaud F, Cadag E, Carlton JM, Cerqueira GC, Creasy T, Delcher AL, Djikeng A, Embley TM, Hauser C, Ivens AC, Kummerfeld SK, Pereira-Leal JB, Nilsson D, Peterson J, Salzberg SL, Shallom J, Silva JC, Sundaram J, Westenberger S, White O, Melville SE, Donelson JE, Andersson B, Stuart KD, Hall N (2005) Comparative genomics of trypanosomatid parasitic protozoa. Science **309**: 404–409

Gao G, Nara T, Nakajima-Shimada J, Aoki T (1999) Novel organization and sequences of five genes encoding all six enzymes for de novo pyrimidine biosynthesis in *Trypanosoma cruzi*. J Mol Biol **285**: 149–161

Gaunt MW, Miles MA (2002) An insect molecular clock dates the origin of the insects and accords with palaeontological and biogeographic landmarks. Mol Biol Evol **19**: 748–761

Gross R, Hacker J, Goebel W (2003) The Leopoldina international symposium on parasitism, commensalism and symbiosis – common themes, different outcome. Mol Microbiol **47**: 1749–1758

Jackson AP, Vaughan S, Gull K (2006) Evolution of tubulin gene arrays in trypanosomatid parasites: genomic restructuring in *Leishmania*. BMC Genomics **7**: 261

Liang XH, Haritan A, Uliel S, Michaeli S (2003) trans and cis splicing in trypanosomatids: mechanism, factors, and regulation. Eukaryot Cell **2**: 830–840

Makiuchi T, Nara T, Annoura T, Hashimoto T, Aoki T (2007) Occurrence of multiple, independent gene fusion events for the fifth and sixth enzymes of pyrimidine biosynthesis in different eukaryotic groups. Gene **394**: 78–86

Marande W, Lukes J, Burger G (2005) Unique mitochondrial genome structure in diplonemids, the sister group of kinetoplastids. Eukaryot Cell **4**: 1137–1146

Martínez-Calvillo S, Nguyen D, Stuart K, Myler PJ (2004) Transcription initiation and termination on *Leishmania major* chromosome 3. Eukaryot Cell **3**: 506–517

Moran NA (2002) Microbial minimalism: genome reduction in bacterial pathogens. Cell **108**: 583–586

Nadeau JH (1989) Maps of linkage and synteny homologies between mouse and man. Trends Genet **5**: 82–86

Nara T, Hashimoto T, Aoki T (2000) Evolutionary implications of the mosaic pyrimidine-biosynthetic pathway in eukaryotes. Gene **257**: 209–222

Nara T, Hirayama-Noguchi Y, Gao G, Murai E, Annoura T, Aoki T (2003) Diversity of aspartate carbamoyltransferase genes of *Trypanosoma cruzi*. Int J Parasitol **33**: 845–852

Nara T, Kamei Y, Tsubouchi A, Annoura T, Hirota K, Iizumi K, Dohmoto Y, Ono T, Aoki T (2005) Inhibitory action of marine algae extracts on the *Trypanosoma cruzi* dihydroorotate dehydrogenase activity and on the protozoan growth in mammalian cells. Parasitol Int **54**: 59–64

Nozaki H, Matsuzaki M, Misumi O, Kuroiwa H, Higashiyama T, Kuroiwa T (2005) Phylogenetic implications of the CAD complex from the primitive red alga *Cyanidioschyzon merolae* (Cyanidiales, Rhodophyta). J Phycol **41**: 652–657

Opperdoes FR, Michels PA (2007) Horizontal gene transfer in trypanosomatids. Trends Parasitol **23**: 470—476

Rodríguez-Ezpeleta N, Brinkmann H, Burger G, Roger AJ, Gray MW, Philippe H, Lang BF (2007) Toward resolving the eukaryotic tree: the phylogenetic positions of jakobids and cercozoans. Curr Biol **17**: 1420—1425

Roy J, Faktorová D, Lukeš J, Burger G (2007) Unusual mitochondrial genome structures throughout the Euglenozoa. Protist **158**: 385—396

Saikia S, Parker EJ, Koulman A, Scott B (2007) Defining paxilline biosynthesis in *Penicillium paxilli*: functional characterization of two cytochrome P450 monooxygenases. J Biol Chem **282**: 16829—16837

Shimodaira H (2002) An approximately unbiased test of phylogenetic tree selection. Syst Biol **51**: 492—508

Shimodaira H, Hasegawa M (2001) CONSEL: for assessing the confidence of phylogenetic tree selection. Bioinformatics **17**: 1246—1247

Simpson AG, Inagaki Y, Roger AJ (2006a) Comprehensive multigene phylogenies of excavate protists reveal the evolutionary positions of "primitive" eukaryotes. Mol Biol Evol **23**: 615—625

Simpson AG, Lukeš J, Roger AJ (2002) The evolutionary history of kinetoplastids and their kinetoplasts. Mol Biol Evol **19**: 2071—2083

Simpson AG, Roger AJ (2004) Protein phylogenies robustly resolve the deep-level relationships within Euglenozoa. Mol Phylogenet Evol **30**: 201—212

Simpson AG, Stevens JR, Lukes J (2006b) The evolution and diversity of kinetoplastid flagellates. Trends Parasitol **22**: 168—174

Stechmann A, Cavalier-Smith T (2003) The root of the eukaryote tree pinpointed. Curr Biol **13**: R665—R666

Sturm NR, Maslov DA, Grisard EC, Campbell DA (2001) *Diplonema* spp possess spliced leader RNA genes similar to the Kinetoplastida. J Eukaryot Microbiol **48**: 325—331

Thompson JD, Higgins DG, Gibson TJ (1994) CLUSTAL W: improving the sensitivity of progressive multiple sequence alignment through sequence weighting, position-specific gap penalties and weight matrix choice. Nucleic Acids Res **22**: 4673—4680

van Ham RC, Kamerbeek J, Palacios C, Rausell C, Abascal F, Bastolla U, Fernández JM, Jiménez L, Postigo M, Silva FJ, Tamames J, Viguera E, Latorre A, Valencia A, Morán F, Moya A (2003) Reductive genome evolution in *Buchnera aphidicola*. Proc Natl Acad Sci USA **100**: 581—586

Yang Z (1997) PAML: a program package for phylogenetic analysis by maximum likelihood. Comput Appl Biosci **13**: 555—556

Young CA, Felitti S, Shields K, Spangenberg G, Johnson RD, Bryan GT, Saikia S, Scott B (2006) A complex gene cluster for indole-diterpene biosynthesis in the grass endophyte *Neotyphodium lolii*. Fungal Genet Biol **43**: 679—693

INTERNAL MEDICINE

□ CASE REPORT □

Pulmonary Paragonimiasis with Coincidental Malignant Mesothelioma

Mariko Yamazaki[1,4], Akihiko Ohwada[1,4], Atsuko Miyaji[1,4], Hiroshi Yamazaki[7], Takeshi Nara[5], Syu Hirai[2], Hiroaki Fujii[6], Toshimasa Uekusa[4], Masaru Suzuki[3], Akihiko Iwase[1,4] and Kazuhisa Takahashi[4]

Abstract

A 72-year-old man patient was referred to our institution for evaluation and treatment of right pleural effusion. Eosinophilic pleural effusion and peripheral eosinophilia were identified during the course of hospitalization. Pulmonary paragonimiasis was confirmed by the presence of paragonimus-specific IgG antibodies for *Paragonimus* (*P.*) *westermani* and *P. miyazakii* in his serum. Although Praziquantel, a highly effective agent for the treatment of lung flukes was repeatedly administered, the pleural effusion did not subside and the patient's condition gradually deteriorated until his death due to circulatory insufficiency. Postmortem examination revealed malignant mesothelioma of the sarcomatous type encasing the right lung and heart. Cardiac involvement accompanied with old and recent-onset myocardial ischemic changes resulted in death of this patient. Here, we report a very rare case of malignant mesothelioma with a concomitant infection of parasitic lung fluke.

Key words: paragonimiasis, malignant mesothelioma, eosinophilia

(Inter Med 47: 1027-1031, 2008)
(DOI: 10.2169/internalmedicine.47.0852)

Introduction

Paragonimiasis, a parasitic infection caused by lung flukes, *Paragonimus* (*P.*) *westermani* and *P. miyazakii* is rarely encountered in Japan but has been a representative parasitic infection of the lungs resulting from the consumption of improperly cooked or raw secondary intermediate hosts containing the parasite, such as fresh water crabs, crayfish and wild boar meat (1). Pulmonary paragonimiasis, cerebral paragonimiasis and subcutaneous paragonimiasis have been previously reported in the literature (2-4). We herein report an elderly Japanese man patient with encapsulated eosinophilic pleural effusion and peripheral eosinophilia diagnosed as paragonimiasis from the positive result of enzyme-linked immunosorbent assay (ELISA) for Paragonimus-specific IgG antibodies. The patient died of cardiac failure without any signs of improvement despite comprehensive and extensive treatment with Praziquantel, a potent anti-parasitic agent. Concomitant malignant mesothelioma was revealed during postmortem examination.

Case Report

A 72-year-old man patient was referred to our institution for evaluation and treatment for right-sided pleural effusion. The patient presented with chief complaints of persistent cough and progressive dyspnea which began approximately two months earlier, as well as right-sided pleural effusion. Thoracentesis performed at his previous hospital revealed

[1]Department of Respiratory Medicine, Juntendo Tokyo Koto Geriatric Medical Center, Tokyo, [2]Department of Pathology, Juntendo Tokyo Koto Geriatric Medical Center, Tokyo, [3]Department of Radiology, Juntendo Tokyo Koto Geriatric Medical Center, Tokyo, [4]Department of Respiratory Medicine, Juntendo University, School of Medicine, Tokyo, [5]Department of Molecular and Cellular Parasitology, Juntendo University, School of Medicine, Tokyo, [6]Department of Pathology, Juntendo University, School of Medicine, Tokyo and [7]Department of Parasitology, Asahikawa Medical College, Asahikawa
Received for publication December 24, 2007; Accepted for publication March 8, 2008
Correspondence to Dr. Mariko Yamazaki, mariko@med.juntendo.ac.jp

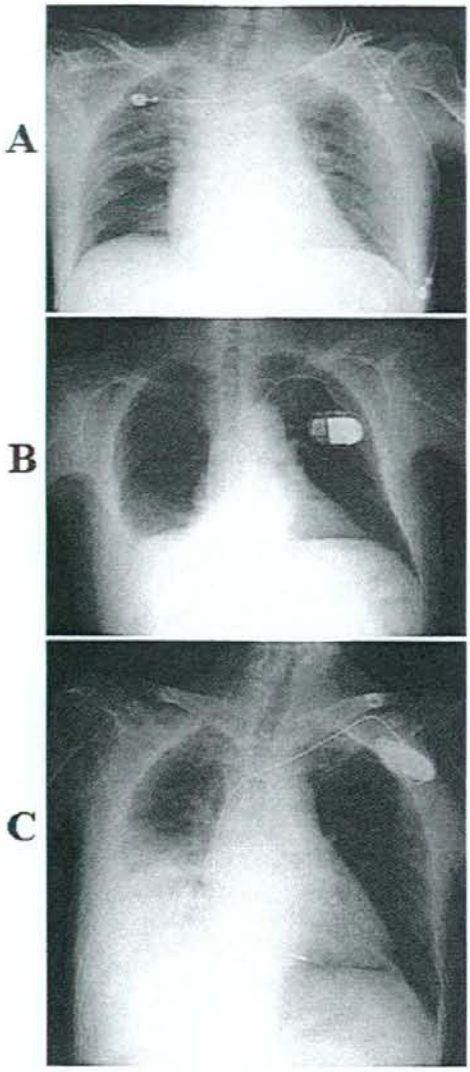

Figure 1. Chest radiographs. Chest radiograph at 16 months prior to admission reveals no sign of pleural effusion or pleural thickening (Panel A). Chest radiograph at 40 days earlier when the time of his admission at the former hospital revealing right pleural effusion and the location of an implanted permanent cardiac pacemaker (Panel B). Chest radiograph taken on admission at our hospital in the Fowler's posture position revealing the deterioration of the patient's right pleural effusion in comparison with his previous radiograph (Panel C).

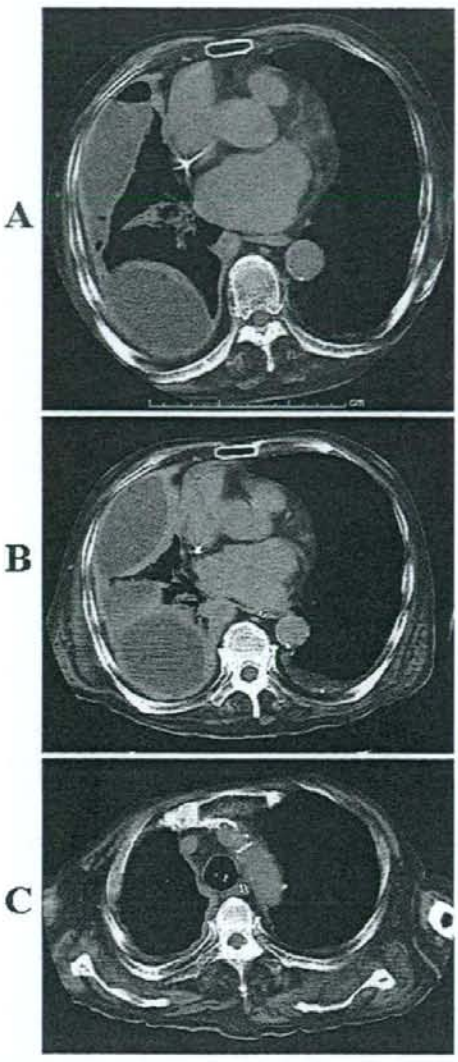

Figure 2. CT of the Thorax. Thoracic CT scan at admission identifying the air-liquid level and the right-sided pleural effusion encapsulated with thickened walls (Panel A). CT scan after the completion of treatment with Praziquantel revealed further deterioration of the plural effusion and an increase in the thickness of the encapsulating wall in comparison to his previous examination (Panel B). In addition, the thickening of the pleural wall extended to the level of right upper lung (Panel C).

characteristic eosinophilic pleural effusion (49% of cells identified were eosinophils). Although no malignant cell or *Mycobacterium tuberculosis* (*M. tuberculosis*) was identified, the level of adenosine deaminase in the pleural effusion was slightly elevated at 40.7 IU/L (normal value, less than 40 IU/L). Systemic administration of prednisolone at the dosage of 15 mg per day and anti-tuberculosis agents, isoniazid (200 mg per day) and rifampicin (300 mg per day) were begun on the suspicion of tuberculous pleuritis. After 40 days of hospitalization without any improvement of accumulation of pleural fluid, the patient was referred and transferred to our institution. Past medical history revealed left-sided hemi-

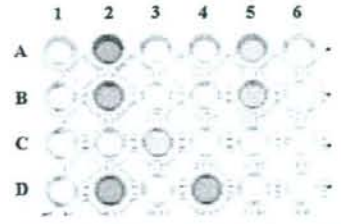

Figure 3. Enzyme-linked immunoabsorbent assay for various parasites. Lanes 1-6 indicate sera obtained from various patients with parasitic infection. Lane 1: serum obtained from negative control patient; lane 2: serum obtained from a patient with *Paragonimus westermani* infection; lane 3: serum obtained from a patient with *Schistosoma mansoni* infection; lane 4: serum obtained from a patient with *Dirofilaria immitis* infection; lane 5: serum obtained from the present case; and lane 6: blank. Rows A-D represent the antigens of various parasites; antigen of *P. westermani* (Row A), *P. miyazakii* (Row B), *S. mansoni* (Row C), *D. immitis* (Row D). The serum of the present case was positive for *P. westermani* (5-A) and *P. miyazakii* (5-B).

plegia resulting from right cerebral infraction secondary to atrial flutter, which had occurred 16 months earlier. Since then, dysphagia and excessive salivation were noted. Brain magnetic resonance imaging was performed in our hospital and an old infarction in the right middle cerebral arterial field was confirmed and there were no additional lesions identified. The patient underwent implantation of a cardiac pacemaker after experiencing multiple episodes of bradycardia due to atrial fibrillation a year ago. His work history revealed that he worked as a ship engineer for one year at age 21 and as a coal miner for 2 years until he finally settled down as an iron welder where he worked for 46 years until he retired at the age of 70 years. Chest radiographic examination performed 16 months earlier revealed no pleural thickening or effusion (Fig. 1A) but the radiographic examination conducted at the time of admission at his former hospital (40 days prior to referral to our hospital) revealed the existence of a right-sided pleural effusion (Fig. 1B). On admission to our hospital, deterioration of the right-sided pleural effusion was noted on the radiographic film (Fig. 1C). Thoracic CT scan revealed right-sided pleural fluid encapsulated with thick walls and an air-liquid level without parenchyma lesions (Fig. 2A). Aspirated pleural effusion revealed exudative straw-colored fluid, pH of 7.22, lactate dehydrogenase of 1,440 IU/L (176 IU/L in serum), protein of 2.6 mg/dL (5.6 mg/dL in serum), glucose of 42 mg/dL (79 mg/dL in serum) and leukocyte count of 3,540 cells/mm^3. Leukocyte differential count was 56.5% lymphocytes, 21.8% eosinophils, 17.7% neutrophils and 4.0% monocytes (mononuclear cells). The level of hyaluronic acid in the pleural fluid was 0.00133 mg/mL (a cut-off level of 75 mg/mL was reported for malignant mesothelioma). Microbiological examination of the aspirated fluid specimen was negative for

Table 1. Peripheral Blood Eosinophil Count

Time: before/after admission at our hospital	Eosinophils (per mm^3)
15 months before	165
12 months before	224
45 days before	844
25 days before	1808
on admission	1755
20 days after	3312
30 days after	8202
40 days after	8278

M. tuberculosis, fungi and bacteria. Repeated cytological examinations of the aspirated fluid were negative for malignant cells. A chest tube was inserted into the right pleural space for the drainage of the pleural effusion when the diagnosis of empyema of unknown etiology was established. Urokinase was administered through the chest tube. On the third day of treatment, overt pneumothorax developed at the right thoracic space. Intra-thoracic administration of urokinase was terminated and the chest tube was kept in place for drainage. However, there was only slight improvement of the hydro-pneumothorax, and the chest tube was removed after 20 days. Then the pleural fluid filled the air space in the thoracic cavity and the pneumothorax was resolved. Tapering of the dosage of prednisolone and the discontinuation of anti-tuberculosis agents were conducted at the time of chest tube placement, and peripheral eosinophilia (defined as eosinophil count of >400 cell/mm^3) became evident (Table 1). The presence of hematological malignancy was omitted from the findings of bone marrow aspiration. Pleural biopsy using a Cope needle revealed the nonspecific inflammation, because the biopsied specimen contained only fibrous proliferation and degenerative mesothelial cells. The serum was examined for the presence of specific IgG antibodies against *Paragonimus westermani*, *Paragonimus miyazakii*, *Schistosoma mansoni* and *Dirofilaria immitis* with enzyme-linked immunosorbant assay (ELISA). The results of ELISA were positive for both *Paragonimus westermani* and *Paragonimus miyazakii* (Fig. 3). Ova for *Paragonimus* were not identified in sputum, pleural fluid or in the stool. The patient recalled eating fried fresh water crabs about 10 years ago but denied recent ingestion of raw or improperly cooked freshwater crab and crayfish or other foods known to harbor the parasite such as wild boar meat. There was no peripheral blood eosinophilia detected 12 months earlier when he underwent surgery for permanent cardiac pacemaker implantation (Table 1). From the positive results of ELISA, we repeatedly administered Praziquantel, orphan drug for treatment of *Paragonimus* with two treatments of 3-day administration at a dose of 3,600 mg (80 mg/kg) per day with an interval of two weeks between treatments. However, there was no improvement in the condition of the pleural fluid. Thoracic CT scan revealed deterioration in pulmonary effusion and thickening of the encasing wall

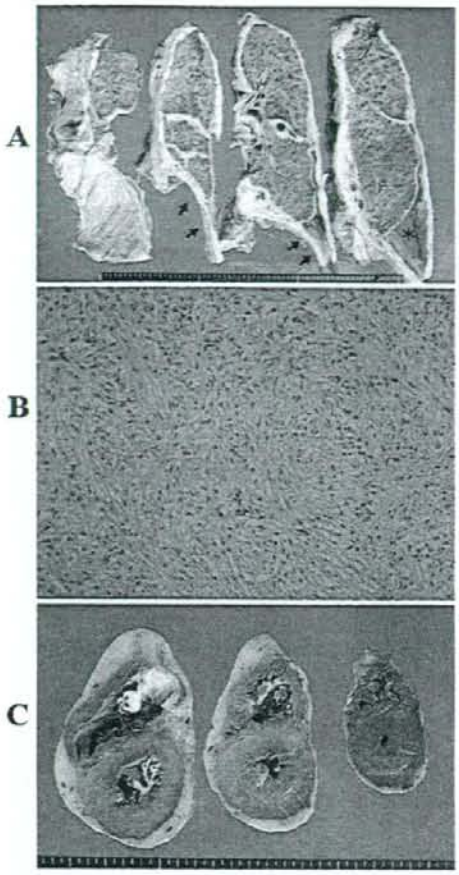

Figure 4. Pathological findings. The gross appearance of right whole lung is encased with thick white-colored fibrous tissue (Panel A). Cavitary lesion is identified in the posterolateral region of the right pleural space (asterisk) (Panel A). Note the right diaphragm was also involved and was diffusely thick (arrows). Microscopic appearance of the tissue encasing the right lung consisted of fibrous sarcomatous tissue stained with Hematoxylin and Eosin staining (Panel B). The gross appearance of heart revealed that the heart was encased with thick fibrous tissue of the malignant mesothelioma, which invaded into the myocardium (Panel C).

(Fig. 2B). Rather the thickness of pleura extended to the level of the superior plane of the lung (Fig. 2C). There were no changes noted for the peripheral eosinophilia at one month (30 days after admission: Table 1). His condition gradually deteriorated until his death on the sixty-seventh day of hospitalization due to progressive congestive heart failure. Postmortem examination was performed. The gross appearance of the right thoracic cavity revealed that the whole right lung was covered with white-colored thick fibrous tissue (Fig. 4A). Hematoxylin and Eosin (HE) staining of the tissue demonstrated the proliferation of spindle-shaped fibrous tumor cells (Fig. 4B). These tumor cells were negative for carcinoembryonic antigen (CEA), epithelioid mesothelioma markers calretinin and mesothelin. However, the tumor cells were positive for vimentin and cytokeratin. The intermediate filament cytoskeleton was also detected with electron microscopy. Together with HE staining and these findings, the pathological diagnosis of sarcomatous type of malignant mesothelioma was made. The heart was encased in a thick layer of malignant mesothelioma with ill-defined margins indicating its invasiveness into myocardium (Fig. 4C). Old and recent onset myocardial necrosis, degenerative changes and scar formation of the heart were also identified. Cardiac involvement by malignant mesothelioma which restricted cardiac motion, together with repeated episodes of ischemic heart disease, were postulated to have resulted in fatal circulatory insufficiency. Pathological characteristics of pulmonary paragonimiasis, such as granuloma formation with or without ova of flukes were not identified in the lungs or pleura.

Discussion

The clinical feature of this patient to be discussed first is the condition of eosinophilia of the pleural fluid. Pleural effusion with greater than 10% eosinophils is often observed in cases with the presence of air or blood in the pleural space, such conditions are encountered after repeated thoracentesis, pneumothorax and traumatic hydrothorax (5). Asbestos-related effusion, pleural effusion secondary to drug reaction or parasitic diseases such as paragonimiasis, malignancy, and tuberculosis are also listed as causes (6). We considered that the prior episode of pneumothorax was rather masked with effusion than *de novo* pneumothorax and drainage with the chest tube clarified the presence of the pneumothorax. We first speculated that air exposure of the pleural space was a causative factor to produce pleural eosinophilia. However, with tapering the dosage of systemically administered steroid, peripheral blood eosinophilia (20 days after admission: Table 1) became evident. Parasitic infection and hematological malignancy are considered to respond to steroid administration. Hematological malignancy was ruled out from the findings of bone marrow aspiration. Spontaneous eosinophilia in peripheral blood associated with mesothelioma is extremely rare (7). Parasitic infection is listed as the top candidate for eosinophilia of pleural effusion and peripheral blood.

The issue to discuss secondly is whether or not pulmonary paragonimiasis was present in this case. Thoracic CT findings of pulmonary paragonimiasis include pulmonary effusion, hydropneumothorax, pulmonary nodules, consolidation, and cysts (8, 9). Pleural involvement without the presence of parenchymal lung lesion as in the present case is often encountered among the known indicated findings (8, 9). There were no parasitic ova identified in the stool, sputum and/or pleural effusion in our case. However, immunoblot analysis for *Paragonimus* specific antibodies is presently the most reliable tool for diagnosis with a sensitiv-

ity of 90% and a specificity of 99% (10). Since ELISA analyses were positive for the presence of antibodies specific to *Paragonimus*, we diagnosed the present case as having pulmonary paragonimiasis with eosinophilic pleural effusion and peripheral eosinophilia.

The latent period between the time of ingestion of contaminated foods and time of appearance of overt symptoms is speculated to be two to three months, although there are much controversies and divergence among clinical reports such as 4, 7, 18 months (11-15). The present patient denied recent ingestion of raw or improperly cooked freshwater crabs, crayfishes, and wild boar meats. Jeon et al reported in their recent article that approximately 30% of the patients in Korea with pulmonary paragonimiasis denied history of eating paratenic hosts (15). As for the treatment of pulmonary paragonimiasis, it is recommended to administer praziquantel at the dose of 75 mg per kilogram for 2 or 3 days. Mukae et al reported that the responsiveness of patients with pulmonary paragonimiasis to praziquantel at this recommended dose is excellent (2) and that all thirteen Japanese patients recovered from pleural effusion. Clinical response in the present case was poor even after two treatments of praziquantel and the final outcome was death due to cardiovascular causes. Cases of paragonimiasis leading to fatal outcomes were observed in patients with cerebral involvement such as cerebral vascular accident and other hemorrhagic consequences (3). Since cerebral involvement was not evident in our case, the clinical course of our patient was considered as a bizarre case for pulmonary paragonimiasis.

Postmortem examination revealed malignant mesothelioma encasing the right pleural space and invading the heart. He had a high risk of malignant mesothelioma with a positive occupational history. Chest radiographic examination taken 16 months earlier was unremarkable; the presence of pleural thickening or effusion was not confirmed, which is often observed in malignant mesothelioma. Since postmortem examination did not reveal any characteristic pathological findings of paragonimiasis such as ova or granulated tissue, we could not speculate whether the infection was fresh or old. However, peripheral blood eosinophilia was evident 45 days before admission (refer to Table 1), suggesting recent infection with paragonimus flukes. This is a very rare case of pulmonary paragonimiasis with coincidental malignant mesothelioma.

Acknowledgement

The authors would like to thank Dr. Tomonobu Okuno of Shin-Katsushika Hospital and Dr. Hitoshi Saitoh of Heisei Tateishi Hospital for their assistance and contribution of the chest radiographs.

References

1. Obara A, Nakamura-Uchiyama F, Hiramatsu K, Nawa Y. Paragonimiasis case recently found among immigrants in Japan. Internal Med **43**: 388-392, 2004.
2. Mukae H, Taniguchi H, Matsumoto N, et al. Clinicoradiologic features of pleuropulmonary *Paragonimus westermani* on Kyusyu Island, Japan. Chest **120**: 514-520, 2001.
3. Choo JD, Suh BS, Lee HS, et al. Chronic cerebral paragonimiasis combined with aneurysmal subarachnoid hemorrhage. Am J Trop Med Hyg **69**: 466-469, 2003.
4. Dainichi T, Nakahara T, Moroi Y, et al. A case of cutaneous paragonimiasis with pleural effusion. Int J Dermatol **42**: 699-702, 2003.
5. Ligh RW. Pleural Diseases. 4th ed. Lippincott Williams & Wilkins, Philadelphia, 2001: 48-50.
6. Martinez-Garcia MA, Cases-Viedma E, Cordero-Rodriguez PJ, et al. Diagnostic utility of eosinophils in the pleural fluid. Eur Respir J **15**: 166-169, 2000.
7. Davis BH. Hypereosinophilia associated with a peritoneal mesothelioma. Arch Pathol Lab Med **103**: 487, 1979.
8. Im JG, Wang HY, Kim WS, Han MC, Shim YS, Chow SY. Pleuropulmonary paragonimiasis: radiologic findings in 71 patients. AJR Am J Roentgenol **159**: 39-43, 1992.
9. Kim TS, Han J, Shim SS, et al. Pleuropulmonary paragonimiasis: CT findings in 31 patients. AJR Am J Roentgenol **185**: 616-621, 2005.
10. Robertson KB, Janssen WJ, Saint S, Weinberger SE. Clinical problem-solving. The missing piece. N Engl J Med **355**: 1913-1918, 2006.
11. Uchida K, Sekiguchi S, Doi Y, Yamazaki H. Pulmonary paragonimiasis with pleural effusion containing paragonimus ova: sonographical appearance of pleural effusion. Intern Med **34**: 1178-1180, 1995.
12. Inoue Y, Kawaguchi T, Yoshida A, et al. *Paragonimiasis miyazakii* associated with bilateral pseudochylothorax. Intern Med **39**: 579-582, 2000.
13. Nakamura-Uchiyama F, Onah DN, Nawa Y. Clinical features of paragonimiasis cases recently found in Japan: parasite-specific immunoglobulin M and G antibody classes. Clin Infect Dis **32**: e 151-e153, 2001.
14. DeFrain M, Hooker R. North American paragonimiasis: case report of a severe clinical infection. Chest **121**: 1368-1372, 2002.
15. Jeon K, Koh WJ, Kim H, et al. Clinical features of recently diagnosed pulmonary paragonimiasis in Korea. Chest **128**: 1423-1430, 2005.

JOURNAL OF CLINICAL MICROBIOLOGY, Jan. 2009, p. 168–174
0095-1137/09/$08.00+0 doi:10.1128/JCM.01573-08

Vol. 47, No. 1

Loop-Mediated Isothermal Amplification Method for Differentiation and Rapid Detection of *Taenia* Species[▽]

Agathe Nkouawa,[1,3]† Yasuhito Sako,[1]†* Minoru Nakao,[1] Kazuhiro Nakaya,[2] and Akira Ito[1]†

Department of Parasitology[1] and Animal Laboratory for Medical Research,[2] Asahikawa Medical College, Midorigaoka Higashi 2-1-1-1, Asahikawa, 078-8510 Hokkaido, Japan, and Medical Research Center, Institute of Medical Research and Medicinal Plants Studies (IMPM), Ministry of Scientific Research and Innovation, Yaoundé, Cameroon[3]

Received 13 August 2008/Returned for modification 14 October 2008/Accepted 6 November 2008

Rapid detection and differentiation of *Taenia* species are required for the control and prevention of taeniasis and cysticercosis in areas where these diseases are endemic. Because of the lower sensitivity and specificity of the conventional diagnosis based on microscopical examination, molecular tools are more reliable for differential diagnosis of these diseases. In this study, we developed and evaluated a loop-mediated isothermal amplification (LAMP) assay for differential diagnosis of infections with *Taenia* species with cathepsin L-like cysteine peptidase (clp) and cytochrome *c* oxidase subunit 1 (cox1) genes. LAMP with primer sets to the cox1 gene could differentiate between three species, and LAMP with primer sets to the clp gene could differentiate *Taenia solium* from *Taenia saginata*/*Taenia asiatica*. Restriction enzyme digestion of the LAMP products from primer set Tsag-clp allowed the differentiation of *Taenia saginata* from *Taenia asiatica*. We demonstrated the high specificity of LAMP by testing known parasite DNA samples extracted from proglottids (n = 100) and cysticerci (n = 68). LAMP could detect one copy of the target gene or five eggs of *T. asiatica* and *T. saginata* per gram of feces, showing sensitivity similar to that of PCR methods. Furthermore, LAMP could detect parasite DNA in all taeniid egg-positive fecal samples (n = 6). Due to the rapid, simple, specific, and sensitive detection of *Taenia* species, the LAMP assays are valuable tools which might be easily applicable for the control and prevention of taeniasis and cysticercosis in countries where these diseases are endemic.

Cestode parasites *Taenia solium*, *Taenia saginata*, and *Taenia asiatica* are the causative agents of taeniasis. Although taeniasis is relatively innocuous, cysticercosis caused by *T. solium* larvae is one of the most severe diseases in humans and remains a complicated health problem in many areas around the world, especially in developing countries (4, 15). Therefore, differentiation of *Taenia* species becomes significant for epidemiological studies and for control of these diseases. Furthermore, it is expected that there are much wider areas in the Asia-Pacific region where the three taeniid species occur sympatrically (3, 5, 23, 24). Diagnosis is mainly performed by microscopic observation of eggs in feces and/or by comparative morphology of proglottids or scolices, but these methods lack both sensitivity and specificity. In order to overcome the lower sensitivity of microscopic diagnosis, various immunological or molecular approaches, including coproantigen and copro-DNA detection methods, have been developed (2, 6, 12, 18, 25). The coproantigen detection method has been shown to be more sensitive than the microscopy method, but it cannot differentiate between *Taenia* species because of it is genus specific, not species specific (2). By contrast, various copro-DNA detection methods using PCR have been developed for sensitive differential detection of taeniid cestodes (6, 12, 18, 25). Although these techniques provide sensitive and reliable diagnostic results, it is not easy to exploit in the laboratories of developing countries where these diseases are endemic, because PCR requires sophisticated equipment, such as a thermal cycler. Furthermore, *Taq* DNA polymerase is often inactivated by inhibitors present in biological samples, which sometimes cause problems for sensitivity and reproducibility (1, 13).

Recently, a novel nucleic acid amplification method termed loop-mediated isothermal amplification (LAMP) has been developed (17). LAMP employs a DNA polymerase with strand displacement activity and four primers that recognize six sequences on the target DNA. This method amplifies DNA with high specificity, sensitivity, and rapidity under isothermal conditions. Since LAMP is done under isothermal conditions (60 to 65°C), simple incubators, such as a water bath or a block heater, are sufficient for DNA amplification (17). Moreover, a large amount of white precipitate of magnesium pyrophosphate is produced as a byproduct, which enables the visual judgment of amplification by a naked eye (14). Hence, LAMP is a highly sensitive and specific DNA amplification tool suitable for the rapid diagnosis of infectious diseases, including parasitic diseases (9, 20, 22), in a well-equipped laboratory and/or small-scale clinical laboratories and is expected to be highly useful and feasible in the field.

In the present study, we developed and evaluated the LAMP assay with a cathepsin L-like cysteine peptidase (clp) gene of nuclear DNA and a cytochrome *c* oxidase subunit 1 (cox1) gene of mitochondrial DNA for differentiation between and rapid diagnosis of infection with *Taenia* species.

* Corresponding author. Mailing address: Department of Parasitology, Asahikawa Medical College, Midorigaoka Higashi 2-1-1-1, Asahikawa 078-8510, Hokkaido, Japan. Phone: 81-166-68-2422. Fax: 81-166-68-2429. E-mail: yasusako@asahikawa-med.ac.jp.
† These authors contributed equally to this work.
▽ Published ahead of print on 12 November 2008.

TABLE 1. *Taenia* species DNA samples used in this study

Taenia species (no. of samples)	Locality	Developmental stage (no. of samples analyzed)
T. saginata (78)	Cambodia	Proglottid (3)
	China	Proglottid (5)
		Cysticercus (1)
	Indonesia	Proglottid (36)
		Cysticercus (12)[a]
	Nepal	Proglottid (2)
	Thailand	Proglottid (9)
	Cameroon	Proglottid (1)
	Ethiopia	Proglottid (2)
	Brazil	Cysticercus (2)
		Proglottid (1)
	Ecuador	Proglottid (1)
	Belgium	Proglottid (2)
		Cysticercus (1)[a]
T. asiatica (43)	China	Cysticercus (1)[a]
		Proglottid (10)
	Indonesia	Cysticercus (2)
		Cysticercus (16)[a]
	Korea	Cysticercus (2)[a]
	Taiwan	Cysticercus (1)[a]
		Proglottid (1)
	Thailand	Proglottid (6)
	Philippines	Proglottid (4)
T. solium (47)	China	Cysticercus (2)
		Proglottid (11)
	India	Cysticercus (11)
	Indonesia	Proglottid (1)
	Nepal	Cysticercus (5)
	Thailand	Proglottid (5)
	Vietnam	Cysticercus (1)
	Cameroon	Cysticercus (3)
	Mozambique	Cysticercus (2)
	South Africa	Cysticercus (1)
	Tanzania	Cysticercus (1)
	Brazil	Cysticercus (1)
	Ecuador	Cysticercus (2)
	Mexico	Cysticercus (1)

[a] The cysticercus was developed in NOD/shi-*scid* mice.

MATERIALS AND METHODS

Parasite materials. Cysticerci of *T. solium*, *T. saginata*, or *T. asiatica* were obtained from nonobese diabetic/severe combined immunodeficiency (NOD/shi-*scid*) mice (7, 16) infected by intraperitoneal cavity injection with oncospheres prepared from gravid proglottids of each parasite isolated in Thailand. Genomic DNA was extracted from one cysticercus by using a DNeasy tissue kit (Qiagen, Hilden, Germany).

DNA samples. For evaluation of the LAMP assay, a total of 168 DNA samples extracted from proglottids (n = 100) and cysticerci (n = 68), including 47 *T. solium* samples, 78 *T. saginata* samples, and 43 *T. asiatica* samples, were examined (Table 1). We used the stored DNA samples previously analyzed by multiplex PCR (25).

Cloning and sequencing of clp genes. The clp gene of each *Taenia* parasite was cloned by PCR with forward primer 5′-ACATTTTCGTTTCGATCGGTCAT G-3′ and reverse primer 5′-TGAACACATGGTTTAAACGTATGG-3′. Primers used were designed from conserved nucleotide sequences between *Echinococcus multilocularis* (21) and *T. solium* (10) clp genes to amplify almost the entire gene region. PCR was carried out using high-fidelity polymerase PrimeStar (Takara, Kyoto, Japan) in a final volume of 25 μl reaction mixture containing 0.2 μM of each primer, 200 μM each of deoxynucleoside triphosphate (dNTP), 0.625 units of PrimeStar DNA polymerase, and genomic DNA, as described above. Amplification was performed with 35 cycles of 94°C for 30 s, 60°C for 15 s, and 72°C for 4 min, followed by a final extension at 72°C for 10 min. A single band of approximately 3 kbp was excised from agarose gels by using a NucleoSpin ExTract kit (Macherey-Nagel, Düren, Germany) according to the instruction manual and was cloned into a pGEM-T vector (Promega, Madison, WI) after the addition of adenine to the ends of the PCR products. The plasmid clone was sequenced on an ABI Prism 310 sequencer (Applied Biosystems, Foster City, CA) with BigDye Terminator version 1.1 (AB Applied Biosystems) and was used as a standard plasmid for determining the specificity and sensitivity of LAMP.

Preparation of standard plasmids for cox1 genes. The cox1 gene of each *Taenia* parasite was amplified by PCR using forward primer 5′-ATGAATGTC AAATATTTGT-TAAGTT-3′ and reverse primer 5′-CTAAAAGACCATTTC ACACGCGAAT-3′ for *T. solium*, forward primer 5′-ATGAGTGTTAAATTT TTATTAAGTT-3′ and reverse primer 5′-TTAAACTAAAAAACCACGGGC AGGC-3′ for *T. saginata*, and forward primer 5′-ATGAGTGTTAAATTTTTA TTAAGTT-3′ and reverse primer 5′-TTAAACTAAAAAACCACGAGCAAA C-3′ for *T. asiatica*. PCR was carried out as described above, except the annealing temperature was at 58°C and the elongation time was 90 s. The amplified products of each *Taenia* species were cloned into a pGEM-T vector and used as a standard plasmid after being confirmed by sequencing.

LAMP primers. LAMP primers were designed using PrimerExplorer V4 software (http://primerexplorer.jp/). The following four oligonucleotide primers were specifically designed to amplify six distinct regions on the target gene: forward inner primer (FIP), backward inner primer (BIP), and two outer primers, F3 and B3 (Table 2). FIP consists of the sense sequence of F2 at the 3′ end and the F1c region at the 5′ end that is complementary to the F1 region. BIP consists of a B2 region at the 3′ end that is complementary to the B2c region and the same sequence as the B1c region at the 5′ end (Fig. 1A and 2A).

LAMP reaction. LAMP was carried out in a 25-μl volume of reaction mixture containing 40 pmol each of FIP and BIP, 5 pmol each of F3 and B3, an 8-U large fragment of *Bst* DNA polymerase (New England Biolabs, Beverly, MA), 20 mM Tris-HCl (pH 8.8), 10 mM KCl, 8 mM $MgSO_4$, 10 mM $(NH_4)_2SO_4$, 0.1% Tween 20, 0.8 M betaine (Sigma, St. Louis, MO), and 1.4 mM each of dNTP and the template DNA. The reaction mixture was incubated for 60 min at 63°C for the clp gene and at 60°C for the cox1 gene and heated at 80°C for 5 min. The LAMP products from primer set Tsag-clp were digested with the HinfI restriction enzyme (New England Biolabs) for 2 h at 37°C. The LAMP products and restriction enzyme-digested products were electrophoresed on a 2.0% agarose gel and detected by staining with ethidium bromide.

Sensitivity analyses. The sensitivities of the LAMP and PCR methods were assessed using a standard plasmid diluted from 10^4 copies/reaction to 1. LAMP was performed as previously mentioned. PCR was carried out by using F3 and B3 primers of each LAMP primer set. PCRs were performed in a 25-μl volume of reaction mixture containing 10 mM Tris-HCl (pH 8.3), 50 mM KCl, 1.5 mM $MgCl_2$, 0.001% gelatin, 0.2 μM of each primer, 0.2 mM each of dNTP, diluted standard plasmid, and 0.5 units of *Taq* DNA polymerase (ExTaq; Takara), and cycling conditions were 30 s at 94°C (first cycle, 2 min at 94°C), 30 s at 60°C (clp gene) and 58°C (cox1 gene), and 30 s at 72°C for 30 cycles. The PCR products were electrophoresed on a 2.0% agarose gel and detected by staining with ethidium bromide.

DNA extraction from fecal samples. In order to evaluate the detection limit of taeniid DNA in fecal samples, 1 gram of feces from a noninfected volunteer was mixed with 5, 10, 20, 30, 40, or 50 *T. asiatica* or *T. saginata* eggs, and DNA was extracted by using a QIAamp DNA stool mini kit (Qiagen) after egg disruption treatment with glass beads (19). In addition, taeniid egg-positive or -negative fecal samples obtained in Indonesia and Thailand were used to assess LAMP, and DNA samples were extracted by the same procedure. LAMP was performed as previously described except that the reaction was performed for 90 min.

Nucleotide sequence accession numbers. The nucleotide sequence data of the clp genes cloned in this study are available in the GenBank, EMBL, and DDBJ databases under accession numbers AB441815 (*T. solium*), AB441816 (*T. saginata*), and AB441817 (*T. asiatica*).

RESULTS AND DISCUSSION

The standard plasmid of each gene was constructed to facilitate initial evaluation and optimization of LAMP. The LAMP products are detected as a ladder of multiple bands on the gel due to the formation of a mixture of stem-loop DNAs with various stem lengths and cauliflower-like structures, with multiple loops formed by annealing between alternately inverted repeats of the target sequence in the same strand (17). Application of the LAMP assay with each specific primer set to each

TABLE 2. LAMP primer sets

Species	Primer set	Primer type[a]	Sequence (5′ to 3′)	Target
T. saginata	Tsag-cox1	F3	TCGGCAAATATTTAATTCCTTTG	cox1 gene
		B3	AAATTCTAGACGCACCCG	
		FIP	GCCATCGAAGGAATCAATAACCAATCTGATTTGAATTTACCCCG	
		BIP	GACTTTTTATCCGCCTTTGTCGTCAATGCAACGAAAACATCAAGA	
T. asiatica	Tasi-cox1	F3	GATTTTCTTTTTTTTGATGCCCA	
		B3	TTGAAAATAATGACGACGACA	
		FIP	AGGCAAGTTTAAATCAGATAACCCATTTTGATAGGTGGTTTTGGTAA	
		BIP	GTGGTTGTTGATTCCTTCAATAGTTTAAGGCGGATAAAAAGTTCAC	
T. solium	Tsol-cox1	F3	CCTATTTTAATTGGAGGTTTTGG	
		B3	CTACCCCACTTCCTCTTGA	
		FIP	CAACCATGCACTTAAAGCATTCAAATTCCATTGATAAGAGGATTATCGG	
		BIP	GGATGTGTTTAGGCGCTGGTACAACGAAGATGATAAAGGTG	
T. saginata	Tsag-clp	F3	GGAAGTCAAAAATCAGGTGAG	clp gene
T. asiatica		B3	CGCTGATAGCTAGGCTAAC	
		FIP	CTCAGTCCCACCCAATCCATTTCAAATCTTCATTATGCTGCGTTAC	
		BIP	GCACCGTGTCATTGGTAAATTTGGTGGAGCTTACTAAGCTCTATCG	
T. solium	Tsol-clp	F3	GAGGTCAAAAATCAGGTGAGAT	
		B3	AATGCTCCTGACTTGGTT	
		FIP	AGGTGCTTTCACAATAGTCCCCTGCGTCATAGGTCTTGC	
		BIP	TAGTCGTTGCTTCGATAGAGCTCGCTGATATCTAGGCTAATGCTG	

[a] FIP consists of the sense sequence of F2 at the 3′ end and the F1c region at the 5′ end that is complementary to the F1 region. BIP consists of a B2 region at the 3′ end that is complementary to the B2c region and the same sequence as the B1c region at the 5′ end.

Taenia cox1 gene resulted in successful amplification of the target gene from the respective parasite genomic DNA (Fig. 1B). On the other hand, because of high nucleotide sequence similarity between the clp genes of *T. saginata* and *T. asiatica*, we could not design a specific primer set to differentiate between these two *Taenia* species but could design specific primer sets Tsol-clp and Tsag-clp to differentiate *T. solium* from *T. saginata* and *T. asiatica* and differentiate *T. saginata*/*T. asiatica* from *T. solium*, respectively. However, the recognition site GAGTC for the restriction enzyme HinfI in the amplified region of the *T. asiatica* clp gene (Fig. 2A) enables us to differentiate *T. asiatica* from *T. saginata*. In this case, restriction enzyme digestion of the LAMP products from *T. asiatica* genomic DNA with primer set Tsag-clp produces three bands with the predicted sizes of 179, 217, and 255 bp, because, unlike the PCR products, the LAMP products are characteristic structures with inverted repeats of the target sequence. In fact, three bands that agreed with the predicted size in the restriction enzyme digestion of the LAMP products from *T. asiatica* genomic DNA with primer set Tsag-clp were detected (Fig. 2B, lane 6).

Analytical specificity of the LAMP assays. In order to evaluate the specificity of the LAMP assays, the known parasite DNA samples prepared from proglottids and cysticerci were examined. Because LAMP requires four primers that recognize six different sequences on a target sequence, the target sequence specificity of the LAMP reaction appears to be high. Indeed, LAMP with primer sets to the cox1 or clp gene specifically amplified each respective target gene, with a species-specific detection. The results obtained by LAMP with cox1 primer sets were consistent with those obtained by multiplex PCR with the cox1 gene, whereas two DNA samples extracted from proglottids, which were identified as being *T. saginata* by both LAMP and multiplex PCR with cox1 primer sets, were detected as *T. asiatica* by LAMP with clp primer sets (Table 3). The size of bands produced by restriction enzyme digestion indicated that these two LAMP products were specifically derived from the *T. asiatica* clp gene (data not shown). After cloning of the clp gene from these two DNA samples by PCR with primer set Tsag-clp F3 and B3 and sequencing, we found a single nucleotide substitution, T to C, as indicated in Fig. 2A, which leads to the appearance of the HinfI recognition site in the region between B1c and B2 and is identical to the nucleotide substitution in *T. asiatica*. Thus, the nucleotide substitution in the clp gene of these two *T. saginata* samples may lead to the different result from the diagnosis based on the cox1 gene. Alternatively, the possibility that these two DNA samples were obtained from a hybrid parasite having *T. asiatica* nuclear DNA and *T. saginata* mitochondrial DNA could not be ruled out, because samples of these parasite materials were collected from areas where both parasites exist sympatrically in China and Thailand, respectively, and these materials were identified by only mitochondrial DNA (3, 8). Exactly two tapeworms obtained in Thailand where three human *Taenia* species were confirmed to be sympatrically occurring (3) are concluded to be the hybrids of *T. saginata* and *T. asiatica* (M. Okamoto, M. Nakao, M. T. Anantaphruti, J. Waikagul, and A. Ito, unpublished data). More-detailed characterizations of these two DNA samples must be performed using another nuclear DNA marker, in addition to analyses of longer nucleotide sequences of the clp genes. These results demonstrated that the LAMP methods with each primer set designed in this study can specifically

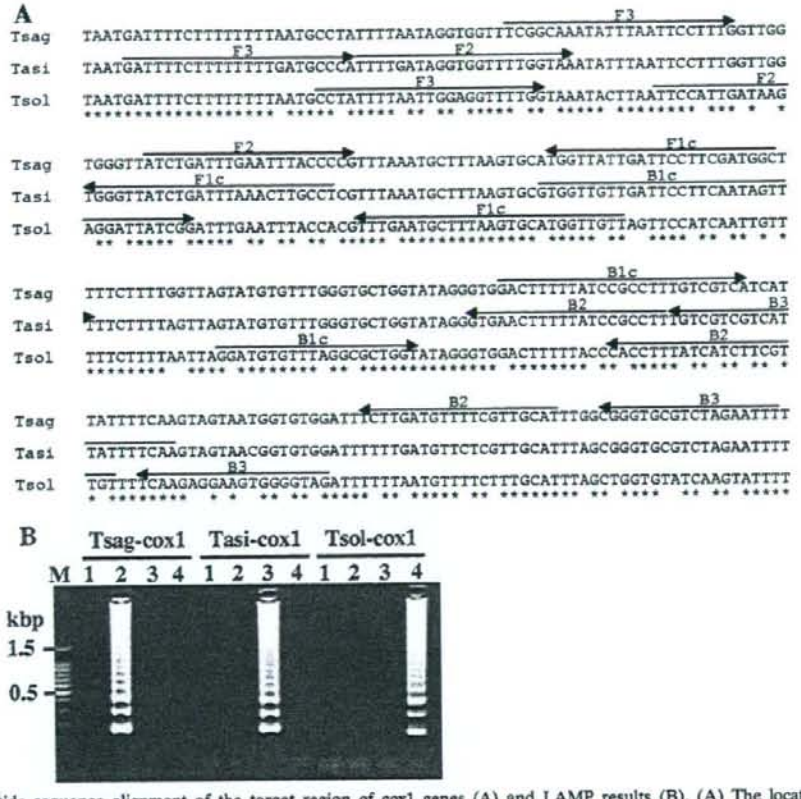

FIG. 1. Nucleotide sequence alignment of the target region of cox1 genes (A) and LAMP results (B). (A) The locations of the primer recognition sites are indicated by arrows. (B) The LAMP products were run on a 2% agarose gel. Lane M, 100-bp DNA ladder marker (Promega); lane 1, negative control; lane 2, *T. saginata* genomic DNA; lane 3, *T. asiatica* genomic DNA; lane 4, *T. solium* genomic DNA; Tsag-cox1, results of LAMP with primer set Tsag-cox1; Tasi-cox1, results of LAMP with primer set Tasi-cox1; Tsol-cox1, results of LAMP with primer set Tsol-cox1.

amplify the target gene and are applicable to a differential diagnosis of infections with *Taenia* species.

Analytical sensitivity of the LAMP assay. Tenfold serial dilution of each standard plasmid was used to determine the lower detection limits for LAMP and PCR, and the sensitivities of the two methods were compared. In this study, F3 and B3 primers of each LAMP primer set were utilized for PCR. Figure 3A shows results of LAMP and PCR with primer set Tsol-clp. Both LAMP and PCR detected up to one copy of target gene/reaction, which indicated no difference in sensitivity between the two methods. LAMP and PCR with other primer sets provided the same results as LAMP with primer set Tsol-clp (data not shown).

Next, the detection limit of taeniid eggs in feces was evaluated using *T. asiatica* and *T. saginata* eggs (Fig. 3B). At least five eggs per gram of feces was sufficient for taeniid eggs to be detected by LAMP with primer sets Tasi-cox1 and Tsag-cox1, whereas more than 10 eggs/g of feces was needed to be detected by LAMP with primer set Tsag-clp (data not shown). The differences between the cox1 gene and the clp gene in the detection sensitivity may be responsible for the number of copies of each target gene within the samples, since a large number of mitochondrial DNA exists in a cell, one feature to be selected as a target DNA for detection. Several detection methods for *Taenia* species in feces based on PCR techniques have been reported. The multiplex PCR method with mitochondrial DNA (25), the PCR-restriction fragment length polymorphism method with mitochondrial DNA (18), and the nested-PCR method with the Tso31 gene encoding the *T. solium* oncosphere-specific protein (12) have been reported to show detection limits of 5 eggs/g of feces, 17 eggs/g of feces, and 40 eggs/g of feces, respectively. It seems that more eggs are needed for detection when the nuclear gene is chosen as a diagnostic gene marker, although the amplification efficiency of each PCR method varies. In this study, *T. solium* eggs were not available, but a similar sensitivity might be expected because all LAMP primer sets could amplify one copy of the target gene when using pure plasmid DNA samples.

Differential detection of *Taenia* species in fecal samples. Furthermore, in order to assess the LAMP method for the detection of copro-DNA, we investigated fecal samples that

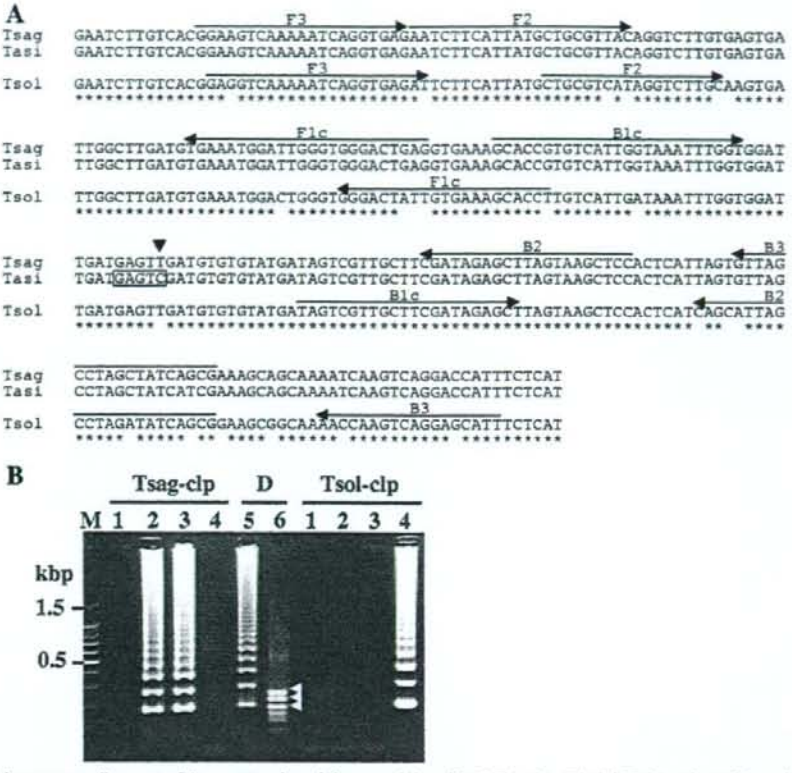

FIG. 2. Nucleotide sequence alignment of the target region of clp genes (A) and LAMP results (B). (A) The locations of the primer recognition sites are indicated by arrows and the restriction enzyme HinfI recognition site in the LAMP products of *T. asiatica* clp gene is boxed. The single nucleotide substitution, C to T, in the *T. saginata* sequence is indicated by an arrowhead. (B) The LAMP products and HinfI digestion products were run on a 2% agarose gel. Lane M, 100-bp DNA ladder marker (Promega); lane 1, negative control; lane 2, *T. saginata* genomic DNA; lane 3, *T. asiatica* genomic DNA; lane 4, *T. solium* genomic DNA; lane 5, HinfI digestion of LAMP products from *T. saginata* genomic DNA with primer set Tsag-clp; lane 6, HinfI digestion of LAMP products from *T. asiatica* genomic DNA with primer set Tsag-clp; Tsag-clp, results of LAMP with primer set Tsag-clp; D, results of HinfI digestion; Tsol-clp, results of LAMP with primer set Tsol-clp. The DNA fragments generated after digestion with HinfI are indicated by arrowheads.

were positive (n = 6) or negative (n = 10) for taeniid eggs by microscopy and collected in Indonesia and Thailand (Fig. 4). Out of six taeniid egg-positive fecal samples, three specimens from Indonesia tested positive with primer sets Tsag-cox1 (Fig. 4A, lanes 15 to 17) and Tsag-clp (data not shown), and the remaining specimens from Thailand were positive with primer sets Tasi-cox1 (Fig. 4B, lanes 12 to 14) and Tsag-clp (data not shown). No differences in detection be-

TABLE 3. Analytical specificity of the LAMP assays[a]

Taenia species (no. of samples)	No. of samples (%) detected by LAMP with indicated primer set	
	cox1	clp
T. saginata (78)	78 (100)	76 (97.4)[b]
T. asiatica (43)	43 (100)	43 (100)
T. solium (47)	47 (100)	47 (100)

[a] *Taenia* species were confirmed by multiplex PCR with cox1 genes (25).
[b] Two samples were detected as *T. asiatica* by LAMP.

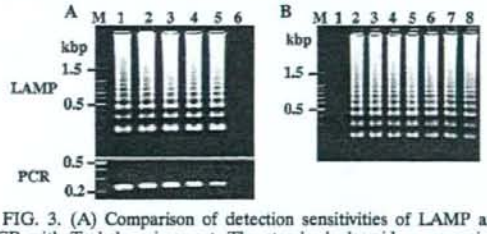

FIG. 3. (A) Comparison of detection sensitivities of LAMP and PCR with Tsol-clp primer set. The standard plasmids were serially diluted from 10^4 copies per reaction to 1 copy per reaction and amplified by LAMP (upper panel) and PCR (lower panel). The F3 and B3 primers of the Tsol-clp primer set were used in the PCR. The LAMP reactions were carried out for 60 min. Lane M, 100-bp DNA ladder marker (Promega); lanes 1 to 5 represent 10^4, 10^3, 10^2, 10, and 1 copy(ies)/reaction, respectively; lane 6, negative control. (B) Detection limits of target genes by LAMP with Tasi-cox1 primer set against DNA samples prepared from feces containing various numbers of *T. asiatica* eggs. The LAMP reactions were carried out for 90 min. Lane M, 100-bp DNA ladder marker; lane 1, negative control; lane 2, *T. asiatica* genomic DNA as a positive control; lanes 3 to 8 represent 5, 10, 20, 30, 40, and 50 *T. asiatica* eggs/g of feces, respectively.

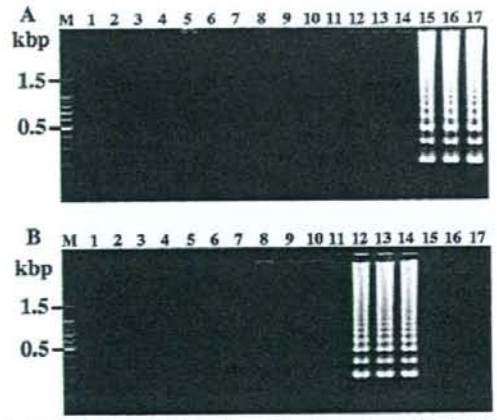

FIG. 4. Differential detection of *Taenia* species in fecal samples. Each genomic DNA extracted from taeniid egg-negative fecal samples collected in Indonesia (lanes 2 to 11) and taeniid egg-positive fecal samples collected in Thailand (lanes 12 to 14) and Indonesia (lanes 15 to 17) was examined by LAMP. The LAMP reactions were carried out for 90 min. The LAMP results with primer sets Tsag-cox1 (A) and Tasi-cox1 (B) are shown. Lane M, 100-bp DNA ladder marker (Promega); lane 1, negative control.

tween nuclear DNA and mitochondrial DNA were observed. The results obtained by LAMP were consistent with those of multiplex PCR. No positive results were observed with the taeniid egg-negative samples.

Our results demonstrated that the LAMP method has high sensitivity and specificity for differential detection of *Taenia* species. Compared to PCR, LAMP has the advantages of reaction simplicity and cost-effectiveness. LAMP does not need sophisticated and expensive equipments, and a simple water bath or a heat block is sufficient to furnish a constant temperature for reactions requiring only 1 to 2 h. Another useful feature of LAMP is that a white precipitate of magnesium pyrophosphate leading to turbidity of reaction mixtures as a byproduct of gene amplification makes it easy to distinguish positive samples from negative samples. In fact, we could discriminate between positive and negative samples by a naked eye in all cases (data not shown). Although limited numbers of clinical specimens were analyzed in the present study, it has been shown that the LAMP method has the potential for use in the differential diagnoses of infections with *Taenia* species that could be easily applicable in countries where taeniasis/cysticercosis are endemic for better control and prevention of these diseases.

ACKNOWLEDGMENTS

Fecal and/or parasite samples used for this study were obtained through joint projects on epidemiological studies of taeniasis/cysticercosis in Indonesia, Thailand, and China (3, 11, 24). We sincerely thank T. Wandra, J. Waikagul, and T. Y. Li for their great help with these samplings.

This work was supported by the leadership in science and technology in Asia from the Ministry of Education, Culture, Sports, Science and Technology, Japan; International Collaboration Research Fund from the Japan Society for the Promotion of Science (JSPS) (17256002); and JSPS-Asia/Africa Science Platform Fund to A.I.

REFERENCES

1. **Abu Al-Soud, W., and P. Rådström.** 2000. Effects of amplification facilitators on diagnostic PCR in the presence of blood, feces, and meat. J. Clin. Microbiol. **38:**4463–4470.
2. **Allan, J. C., G. Avila, J. Garcia-Noval, A. Flisser, and P. S. Craig.** 1990. Immunodiagnosis of taeniasis by coproantigen detection. Parasitology **101:** 473–477.
3. **Anantaphruti, M. T., H. Yamasaki, M. Nakao, J. Waikagul, D. Watthanakulpanich, S. Nuamtanong, W. Maipanich, S. Pubampen, S. Sanguankiat, C. Muennoo, K. Nakaya, M. O. Sato, Y. Sako, M. Okamoto, and A. Ito.** 2007. Sympatric occurrence of *Taenia solium*, *T. saginata*, and *T. asiatica*, Thailand. Emerg. Infect. Dis. **13:**1413–1416.
4. **Bern, C., H. H. Garcia, C. Evans, A. E Gonzalez, M. Verastegui, V. C. W. Tsang, and R. H. Gilman.** 1996. Magnitude of the disease burden from neurocysticercosis in a developing country. Curr. Infect. Dis. **29:**1203–1209.
5. **Eom, K. S., H. K. Jeon, Y. Kong, U. W. Hwang, Y. Yang, X. Li, L. Xu, Z. Feng, Z. S. Pawlowski, and H. J. Rim.** 2002. Identification of *Taenia asiatica* in China: molecular, morphological, and epidemiological analysis of a Luzhai isolate. J. Parasitol. **88:**758–764.
6. **González, L. M., E. Montero, L. J. S. Harrison, R. M. E. Parkhouse, and T. Garate.** 2000. Differential diagnosis of *Taenia saginata* and *Taenia solium* infection by PCR. J. Clin. Microbiol. **38:**737–744.
7. **Ito, A., K. Nakaya, Y. Sako, M. Nakao, and M. Ito.** 2001. NOD-*scid* mouse as an experimental animal model for cysticercosis. Southeast Asian J. Trop. Med. Public Health **32:**85–89.
8. **Ito, A., M. Nakao, T. Wandra, T. Suroso, M. Okamoto, H. Yamasaki, Y. Sako, and K. Nakaya.** 2005. Taeniasis and cysticercosis in Asia and the Pacific: present state of knowledge and perspectives. Southeast Asian J. Trop. Med. Public Health **36:**123–130.
9. **Kuboki, N., N. Inoue, T. Sakurai, F. D. Cello, D. J. Grab, H. Suzuki, C. Sugimoto, and I. Igarashi.** 2003. Loop-mediated isothermal amplification for detection of African trypanosomes. J. Clin. Microbiol. **41:**5517–5524.
10. **Li, A. H., S. U. Moon, Y. K. Park, B. K. Na, M. G. Hwang, C. M. Oh, S. H. Cho, Y. Kong, T. S. Kim, and P. R. Chung.** 2006. Identification and characterization of a cathepsin L-like cysteine protease from *Taenia solium* metacestode. Vet. Parasitol. **141:**251–259.
11. **Li, T., P. S. Craig, A. Ito, X. Chen, D. Qiu, J. Qiu, M. O. Sato, T. Wandra, H. Bradshaw, L. Li, Y. Yang, and Q. Wang.** 2006. Taeniasis/cysticercosis in a Tibetan population in Sichuan province, China. Acta Trop. **100:**223–231.
12. **Mayta, H., R. H. Gilman, E. Prendergast, J. P. Castillo, Y. O. Tinoco, H. H. Garcia, A. E. Gonzalez, and C. R. Sterling.** 2008. Nested PCR for the specific diagnosis of *Taenia solium* taeniasis. J. Clin. Microbiol. **46:**286–289.
13. **Monteiro, L., D. Bonnemaison, A. Vekris, K. G. Petry, J. Bonnet, R. Vidal, J. Cabrita, and F. Mégraud.** 1997. Complex polysaccharides as PCR inhibitors in feces: *Helicobacter pylori* model. J. Clin. Microbiol. **35:**995–998.
14. **Mori, Y., K. Nagamine, N. Tomita, and T. Notomi.** 2001. Detection of loop-mediated isothermal amplification reaction by turbidity derived from magnesium pyrophosphate formation. Biochem. Biophys. Res. Commun. **289:**150–154.
15. **Murell, K. D.** 2005. Epidemiology of taeniasis and cysticercosis, p. 32–44. *In* K. D. Murell (ed.), WHO/FAO/OIE guidelines for the surveillance, prevention and control of taeniasis/cysticercosis. OIE, Paris, France.
16. **Nakaya, K., W. Mamuti, N. Xiao, M. O. Sato, T. Wandra, M. Nakao, Y. Sako, H. Yamasaki, Y. Ishikawa, P. S. Craig, P. M. Schantz, and A. Ito.** 2006. Usefulness of severe combined immunodeficiency (scid) and inbred mice for studies of cysticercosis and echinococcosis. Parasitol. Int. **55**(Suppl.):S91–S97.
17. **Notomi, T., H. Okayama, H. Masubuchi, T. Yonekawa, K. Watanabe, N. Amino, and T. Hase.** 2000. Loop-mediated isothermal amplification of DNA. Nucleic Acids Res. **28:**e63.
18. **Nunes, C. M., A. K. K. Dias, F. E. F. Dias, S. M. Aoki, H. B. D. Paula, L. G. F. Lima, and J. F. Garcia.** 2005. *Taenia saginata*: differential diagnosis of human taeniasis by polymerase chain reaction-restriction fragment length polymorphism assay. Exp. Parasitol. **110:**412–415.
19. **Nunes, C. M., L. G. F. Lima, C. S. Manoel, R. N. Pereira, M. M. Nakano, and J. F. Garcia.** 2006. Technical report: fecal specimens preparation methods for PCR diagnosis of human taeniosis. Rev. Inst. Med. Trop. Sao Paulo **48:**45–47.
20. **Poon, L. L. M., B. W. Y. Wong, E. H. T. Ma, K. H. Chan, L. M. C. Chow, W. Abeyewickreme, N. Tangpukdee, K. Y. Yuen, Y. Guan, S. Looareesuwan, and J. S. M. Peiris.** 2006. Sensitive and inexpensive molecular test for falciparum malaria: detecting *Plasmodium falciparum* DNA directly from heat-treated blood by loop-mediated isothermal amplification. Clin. Chem. **52:**303–306.
21. **Sako, Y., H. Yamasaki, K. Nakaya, M. Nakao, and A. Ito.** 2007. Cloning and characterization of cathepsin L-like peptidases of *Echinococcus multilocularis* metacestodes. Mol. Biochem. Parasitol. **154:**181–189.
22. **Savan, R., T. Kono, T. Itami, and M. Sakai.** 2005. Loop-mediated isothermal